Dedicated to innovation in aerospace

OPZuid
Europees Innovatieprogramma Zuid-Nederland

Provincie Noord-Brabant

Europese Unie
Europees Fonds voor Regionale Ontwikkeling

PUBLIC

NLR-CR-2019-513-RevEd-1 | July 2023

Evaluation on in-service laser shearography for composite structures

WP2 NDI (Non-destructive Inspection) in-service

CUSTOMER: OPZuid (Operationeel Programma Zuid-Nederland)

Royal NLR - Netherlands Aerospace Centre

Dedicated to innovation in aerospace

Evaluation on in-service laser shearography for composite structures

WP2 NDI (Non-destructive Inspection) in-service

REPORT NUMBER
NLR-CR-2019-513-RevEd-1

AUTHOR(S)
E.R. Rademaker
H.P. Jansen
R.B.R.T. Lambrichs

REPORT CLASSIFICATION
ONGERUBRICEERD

DATE
July 2023

KNOWLEDGE AREA(S)
Testen van vliegtuigconstructies en -materialen
Levensduurbewaking en onderhoud van vliegtuigen

DESCRIPTOR(S)
Non-destructive Inspection (ndi)
Shearography
Composites
In-service
MRO

Problem area

The application of novel maintenance methods and availability of more accurate operational information is of key importance for the further reduction of aircraft down time, direct maintenance costs, predictability of aircraft availability and the everlasting need to improve price-performance ratio of aircraft operations and maintenance. Non-Destructive Inspection (NDI) is a vital link during Maintenance Repair and Overhaul (MRO) and further development of emerging inspection methods is crucial to keep maintenance efficient and cost effective. Within the framework of the Development Composite Maintenance Centre (DCMC), part of an OPZuid project, the novel NDI methods are further developed within Work Package 2 (WP2) to pursue this goal. Further, NLR knowledge, acquired within a broader multiannual framework, w.r.t. NDI is being used in WP2. The objective of WP2 is the development of reliable, fast and automated NDI method for large composite surface areas. Previous study, performed by the NLR, presented an overview of promising NDI methods which fulfils the objective of WP2. The down selection of NDI methods was based on technical characteristics and commercial aspects.

Description of work

Shearography was evaluated as a promising technique because of the non-contact nature, portability, fast operation, large Field Of View FOV (~1m^2), single sided access, all-in-all well suited for in-service inspections. The shearography method was evaluated on a thermoset material comprising a carbon composite solid and a sandwich laminate including the following damage types; impact damage, foil delaminations and skin-to-core disbonds. This report gives the results of an evaluation of the shearography method for in-service inspection of aircraft structures.

Results and conclusions

The assumptions of the research study are confirmed in this investigation. It is confirmed that the shearography inspection method is portable enough to operate under hangar conditions, operates fast, non-contact, has a large FOV (~1m^2), only needs a single sided access and is therefore well suited for in-service inspections. The method is only suitable for relative thin composite structures up to about 5-6 mm, depending on the acceptance criteria. The method is well capable of detecting impact damage, which is the most severe in-service damage that can occur to a composite structure. Inserted Teflon foils could not be detected. Possible reason that the foils are not detected, is that the foils are adhered to the adjacent composite layers instead of a full separation of the individual laminate layers. This does not alter the local stiffness of the component, resulting in zero detectability. All skin-to-core disbonds (> ¼ inch) could be detected reliably, actually the shearograpy inspection method is highly suited for this defect type. Summarizing, shearography is a cost effective inspection method for first screening of large composite areas for both solid and sandwich structures. When more detailed information is needed, other NDI techniques can be used on the anomalous areas.

Applicability

This study has shown that the shearography method is a complementary NDI method and very well suitable to perform in-service inspections under hangar conditions. This result provides DCMC partners direction to further develop shearography inspection methods for composite in-service inspection.

Royal NLR
Anthony Fokkerweg 2
1059 CM Amsterdam, The Netherlands
p) +31 88 511 3113
e) info@nlr.nl i) www.nlr.nl

Dedicated to innovation in aerospace

OPZuid
Europees Innovatieprogramma Zuid-Nederland

Provincie Noord-Brabant

Europese Unie
Europees Fonds voor Regionale Ontwikkeling

PUBLIC

NLR-CR-2019-513-RevEd-1 | July 2023

Evaluation on in-service laser shearography for composite structures

WP2 NDI (Non-destructive Inspection) in-service

CUSTOMER: OPZuid (Operationeel Programma Zuid-Nederland)

AUTHOR(S):

E.R. Rademaker	NLR
H.P. Jansen	NLR
R.B.R.T. Lambrichs	NLR

Royal NLR - Netherlands Aerospace Centre

CUSTOMER	**OPZuid (Operationeel Programma Zuid-Nederland)**
CONTRACT NUMBER	**31B1.0730 (PROJ-007230)**
OWNER	**NLR**
DIVISION NLR	**Aerospace Vehicles**
DISTRIBUTION	**Unlimited**
CLASSIFICATION OF TITLE	**UNCLASSIFIED**

APPROVED BY:		**Date**
AUTHOR	H.P. Jansen	06-07-2023
REVIEWER	D.J. Platenkamp	10-07-2023
MANAGING DEPARTMENT	P. Arendsen	11-07-2023

Summary

The application of novel maintenance methods and availability of more accurate operational information is of key importance for the further reduction of aircraft down time, direct maintenance costs, predictability of aircraft availability and the everlasting need to improve price-performance ratio of aircraft operations and maintenance. Non-Destructive Inspection (NDI) is a vital link during Maintenance Repair and Overhaul (MRO) and further development of emerging inspection methods is crucial to keep maintenance efficient and cost effective. Within the framework of the Development Composite Maintenance Centre (DCMC), part of an OPZuid project, the novel NDI methods are further developed within Work Package 2 (WP2) to pursue this goal. Further, NLR knowledge, acquired within a broader multiannual framework, w.r.t. NDI is being used in WP2. The objective of WP2 is the development of reliable, fast and automated NDI method for large composite surface areas.

A research study was performed by the NLR [1] to get an overview of promising NDI methods which satisfy the requirements established in WP2. The down selection of NDI methods was based on the following inspection characteristics: the performance for defect detection, characterisation of the defects (size and depth), portability of the equipment, Field Of View (FOV), automatization/inspection speed, safety issues and costs of the equipment. The following NDI methods were selected for further evaluation: Laser Ultrasonic (LU), Infrared Thermography (IRT), laser shearography and X-ray backscatter technique. For LU testing, a round robin test will be performed within WP2 evaluating equipment's from different manufactures [2]. For thermography, an evaluation of the NDI methods is performed by the NLR [3]. This report provides the results of an evaluation of laser shearography method for in-service inspection of aircraft structures. From a technical point of view the X-ray backscatter technique is an interesting technique. However, the current equipment costs (ROM > 500,- k€) are considered too high to fulfil the requirements of a cost effective inspection.

The evaluation of shearography has been conducted on two composite reference panels (monolithic and sandwich), containing artificial defects (foils and disbonds) and natural impact damages. The evaluation of shearography showed, that the method is well capable of detecting impact-induced damage. Additionally, the method is highly suited to detect skin-to-core disbonds in sandwich structures. The technique is not able to detect Teflon inserts into the composite skin. The Teflon inserts simulate a delamination for ultrasonic inspection, but not for shearography since the tapes are still adhered to the layers of the skin which does not result in a different response under thermal excitation.

Shearography equipment is relatively portable and it operates contactless. Furthermore, it has a large FOV (~1 m^2) and it only requires a single sided access. Therefore, shearography is well suited for in-service inspections. Care should be taken to avoid excessive vibrations during measurement.

Contents

Abbreviations

ACRONYM	DESCRIPTION
CCD	Charged Coupled Device
ESPI	Electronic Speckle Pattern Interferometry
ESPSI	Electronic Speckle Pattern Shearing Interferometry
InHolland	InHolland University of Applied Sciences Delft
MRO	Maintenance, Repair and Overhaul
NLR	Royal NLR - Netherlands Aerospace Centre

NAME	DESCRIPTION	UNIT
A	amplitude of light signal to camera	-
I	light intensity	-
k	wave number	1/m
s_i	light signal to camera	-
t	time	s
T	time period	s
u,v,w	displacements	m
x,y,z	co-ordinates	m
ε	strain component	-
φ	phase of time signal or phase of shearogram	deg
γ	contrast	-
λ	wave length	m

1 Introduction

The Development Centre for Maintenance of Composites (DCMC) has started in 2016 at industry park Aviolanda situated in Woensdrecht. The objective of DCMC is to cluster knowledge with respect to Maintenance Repair and Overhaul (MRO) of composite structures. The DCMC research program consists of seven Work Packages (WP), containing topics with respect to composite repair and inspection:

- WP1: Patchbond “development and certifying of composite bonded repair”
- WP2: Non-Destructive Inspection (NDI), in-service
- WP3: Improved rotor blade balancing
- WP4: Non-Destructive Inspection (NDI), thick composite structures
- WP5: Field & onsite repairs of composite structures
- WP6: Automated laser preparation for a composite bonded repair
- WP7: Fieldlab organisation and facilities

A research study was performed by the NLR [1] to get an overview of promising Non-Destructive Inspection (NDI) methods which satisfy the requirements stated in WP2. The down selection of NDI methods was based on the following inspection characteristics: the performance for defect detection, characterisation of the defects (size and depth), portability of the equipment, Field Of View (FOV), automatization/inspection speed, safety issues and costs of the equipment. The following NDI methods were selected for further evaluation: Laser Ultrasonic (LU), Infrared Thermography (IRT), laser shearography and X-ray backscatter technique. For LU testing, a round robin test is performed within WP2 evaluating equipments from different manufactures [2]. For thermography, an evaluation of the NDI methods is performed by the NLR [3].This report provides the results of an evaluation of the shearography method for in-service inspection of aircraft structures. Although from a technical point of view the X-ray backscatter technique is an interesting technique the current equipment costs are considered too high (ROM > 500,- k€) to fulfil the requirements of a cost effective inspection. Table 1 shows an overview of the performance of the selected NDI methods.

Table 1: Overview of the performance of the selected NDI methods [1]

Inspection Characteristic		**NDI methods**			
		Laser UT	**IR thermography**	**Laser shearography**	**X-Ray backscatter**
Defect detection	Impact	++	+	+	+
	Delamination / disbond	++	+[1]	0[1]	0[2]
	Kissing bond	0[3]	-	-	-
	Water ingress	0	+	-	+
Defect sizing		++	+	+	+
Depth estimation		++	0[4]	-	-
Portability equipment		-	0	0	-
Field Of View		+[5]	+	0	0
Inspection speed		+	++	+	+
Safety aspects		0	+	0	-
Investment costs		> 500 k€[6]	< 500 k€	< 500 k€	> 500 k€

The colours in the table give a rough qualification of the evaluation parameters for the different NDI methods (green – positive, yellow – with limitation, red – negative).
Note: 1 – for relative thin material (thickness < 5 mm), 2 – orientation depended w.r.t. the X-ray beam, 3 – non-linear UT or UT frequency analyses, 4 – TSR or PPT technology, 5 – using scan system, 6 – trending less expensive equipment in development

This report gives the results of an evaluation of using shearography for the in-service inspection of composite structures. As a start, an internship was defined and a student of the InHolland University of Applied Sciences in Delft, Rik Lambrichs, carried out his practical work based on the research objective and questions posed hereafter.
A main research question for the internship has been formulated:

To what extent is the NDT-technique shearography suitable for future multi-domain aerospace maintenance (MRO) on composite parts?

In order to answer above main question, a series of sub research questions have been formulated:

1. *What are the main theoretical benefits of shearography compared to other means of NDT currently used in aerospace?*
2. *What are the requirements for shearography to be of sufficient added value?*
3. *What are the most suitable testing conditions for shearography, with the possible future user in mind?*
4. *What are the practical capabilities of shearography when looking at various composite material properties and different types of defects?*
5. *Which of the theoretical benefits of shearography can be retraced from the practical research?*

The results of the experimental work during the internship are reported in [4]

Additionally, following the internship the damage detection and quantification characteristics will be evaluated by means of two reference panels.

Chapter 2 starts by first defining the relevant in-service defects that can be found in a composite structures. Chapter 3 gives an introduction to laser speckle pattern interferometry while chapter 4 gives more background on shearography. The equipment used for the inspection is described in chapter 5. The specification of the test samples used in this work is described in chapter 6. The results and discussion of the test samples is presented in chapter 7. An additional chapter stating the results of the internship are presented in Chapter 8 and the conclusions of this work are presented in Chapter 9.

2 Definition of in-service damage

In general it can be observed that Carbon Fiber Reinforced Polymers (CFRP) are widely used in light-weight structures. From the aerospace point of view, the new aircraft types, such as F-35, NH-90, B787 and A350, are examples of large-scale application of CFRP. Moreover, other non-aerospace sectors, e.g. the automotive, maritime, civil engineering, energy (wind turbines) and infrastructure, show trending of increased CFRP applications for its light weight structures. Due to this increase of need for CFRP materials, demand for fast and cost-effective NDI techniques during in-service of the component also increases. To select the appropriate NDI technique, it is important to know what kind of damage types can occur during the service life of a component. Table 2 gives an overview of typical defect types which can occur in composite material during the different stages of the manufacturing process and in-service life. For the in-service inspection of a composite structure, knowledge of the production process and the end product is essential, especially the defect types, which can be present in an accepted composite structure. The last column gives the overview of the defect types which can occur during service life of a composite structure. Especially delamination (e.g. caused by Foreign Object Damage (FOD)) is a relevant defect type because impact damage is generally considered as the type of in-service damage most significantly affecting the structural strength.

Table 2: Typical defect types composite material

Typical defect types composite material			
Incoming material:	During manufacturing	Final composite structure	In-service defects
Contaminations	Contaminations	Delamination	Delamination
Damaged filaments	Damaged filaments	Edge defects	Edge defects
Fiber misalignment	Edge fraying	Foreign object	Disbond
Fuzz balls	Fiber misalignment	In-plane fibre waviness	Kissing bond
Gaps	Fuzz balls	Micro cracks	Surface defects
Missing roving	Gaps	Out-of-plane fibre waviness	Water ingress
Warp deviation	Missing roving	Porosity	
Weft deviation		Resin rich areas	
Skewing		Surface defects	
Crease, wrinkle, wavy cloth		Void	
Broken filaments Local fiber or weave distortions, Fuzz balls, broken selvedge			
Yarn splices (Warp/Weft)			
Excess binder, binder gaps			

3 Introduction to laser speckle pattern interferometry

Laser speckle interferometry makes use of the intensity distribution pattern formed from space interference, generated by illumination of coherent light onto rough object surfaces (Figure 1). Laser speckle interferometry is an effective NDT technology with advantages of non-contact, the illumination over the surface of the object need not be uniform, high sensitivity and detection rate. It has been widely used in many industry areas. Laser speckle interferometry can be used in inspection of metal, ceramic, glass, rubber and composite materials. The surface stress can be also measured for highly accurate measurements of deformation, which means it has great application potential in aerospace, automotive, marine and high-tech materials manufacture.

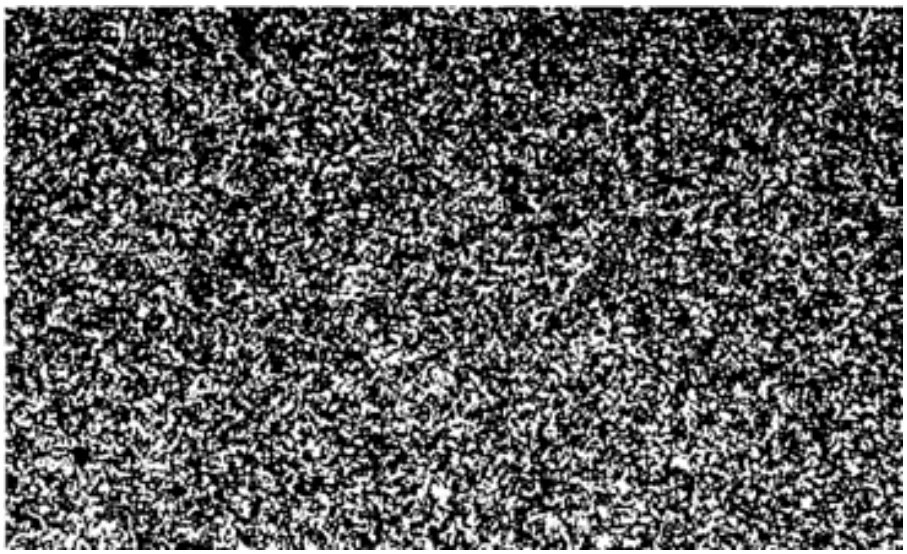

Figure 1: Typical speckle pattern from [5]

In the laser speckle interferometer field, the two most important technologies are:

1. ESPI (Electronic Speckle Pattern Interferometry) and
2. ESPSI (Electronic Speckle Pattern Shearing Interferometry).

3.1 EPSI

Electronic Speckle Pattern-Interferometry (ESPI) combines double ray interference technology with digital recording devices, and can be classified as in-plane ESPI and out-of-plane ESPI. Take the out-of-plane ESPI as the example, with the operating principle shown in Figure 2. The object light reflected by object surfaces superimposes with the reference light which directly emits into CCD target, forming double ray interference patterns. ESPI is a whole-field optical technique widely used for measuring displacement components, shape and slope contours of surfaces, etc. This non-contact and highly sensitive technique has developed into a powerful online inspection tool for non-destructive evaluation. The salient feature of ESPI is its capability to display the correlation fringes in real time on a TV monitor without the need of photographic processing or optical filtering. In conventional ESPI applications the displacement of the laser speckle is used to study the displacement of object surface. This method used charge-coupled device (CCD) or complementary metal oxide semiconductor (CMOS) cameras to record the object speckle

before and after force is applied; and then electronically process and compare the measurements; similar to interference fringes, the final results will be display in the TV screen.

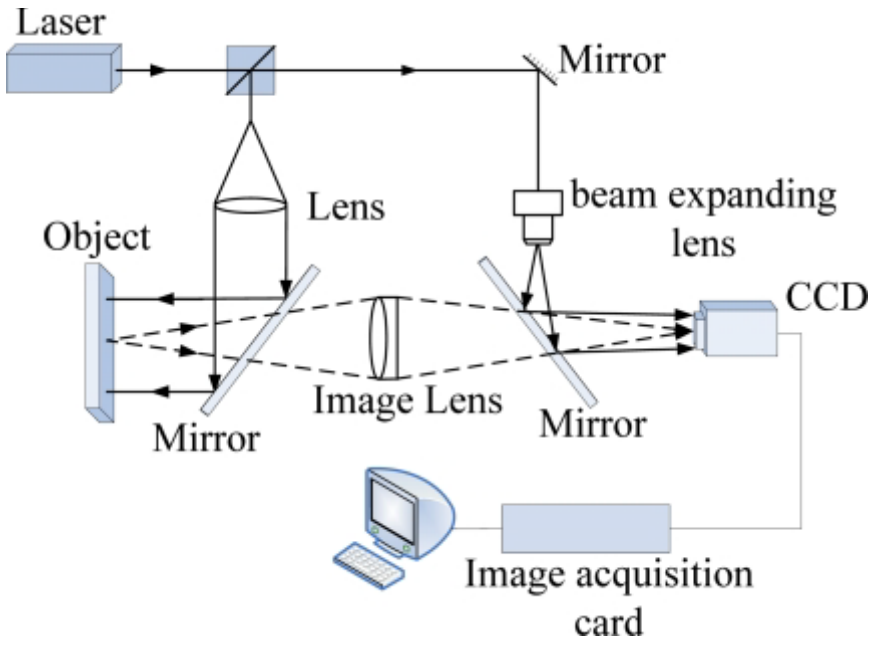

Figure 2: Electronic Speckle Interferometry (ESPI) system [6]

3.2 ESPSI

In order to improve the anti-seismic performance of ESPI, in 1989 Hung [7] employed staggered technology and proposed the concept of ESPI dislocation (Electronic Shearography). Main driver for the development of this technique is to determine the displacement gradients values in various directions (out of plane and in-plane). This technique has been widely used in NDT for in-line quality control and tracking. Electronic speckle pattern shearing interferometry (ESPSI), also known as digital shearography, is a full-field non-destructive, optical technique used to measure approximately the field of displacement derivatives. It can be divided into out-of-plane displacement gradient measurement, in-plane displacement gradient measurement, and multi-component measurement. The operating principle of the out-of-plane displacement gradient measurement system is shown in Figure 3. A laser illuminates the object after passing through a beam expander mirror, and the diffuse reflected light splits into two beams at the splitter. The two beams are reflected by the reflecting mirrors and then get focused by the images lens onto the image plane of the imaging system. As shown in Figure 3, Michaelson interferometer can be used for image shearography. Tilting of one of the shear reflecting mirror will cause the two speckles in the image plane to shear each other, and the two sheared speckles superimpose to form the speckle interference patters, which is recorded by the CCD camera. Deformation of the object will also cause the speckle pattern to change. Shearography uses CCD camera to digitize the speckle patterns before and after the object deformation, which is then processed by computer, as shown by Figure 3(b) (the white horizontal line is added by author). The difference of the two speckle patterns would reproduce the strap pattern in the shear direction which corresponds to the derivative of the displacement, and therefore the object deformation is measured.

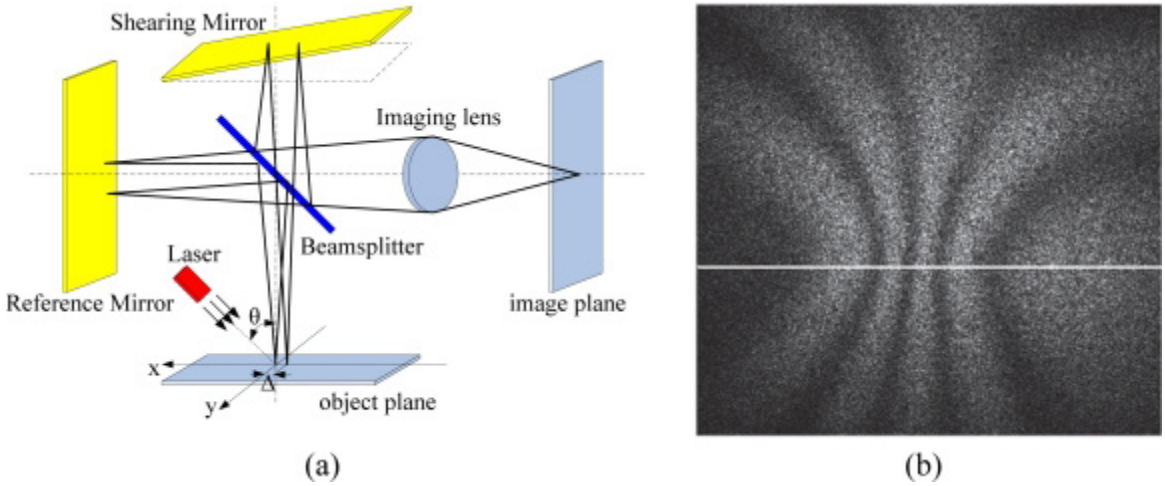

Figure 3: Electronic Speckle Shearing Interferometry (ESPSI) system [6]. (a) Out-of-plane Electronic Shearography; (b) A shearography correlation fringe pattern

This method directly measures the surface deformation gradient, with precise phase shifting and image analysis, it has advantages of real-time testing with post-processing of digital results. Moreover, it is less affected by the object rigid body dynamics and the results are reliable. Testing results can quickly show on the screen, and can represent the defect size by accurately quantify the bending strain.

Shearography and ESPI systems are full-field optical techniques that can be used for out-of-plane contour and slope measurements. ESPI measures surface profiles directly, while shearography measures gradients of the slopes.
For those objects without planar shapes, contours and slopes are required for a complete surface strain analysis.
Summarizing, the difference result between ESPI and ESPSI measurement, displacement versus displace derivative/gradient, is caused by the different nature of the reference beam: ESPI internal reference beam in optical system and ESPSI reference beam radiated from the object surface, which is correlated to the signal beam radiated from the object surface.

4 Background theory of shearography

It is noted that the content of this chapter is somewhat more elaborated than the features of the used Edevis equipment. Additionally and for completeness, some details of shearographic in-plane gradient measurements are given. The tests and results however are confined to the measurements of the out-of-plane displacements of the samples under investigation.

ESPSI is based on taken the interference patterns on a reference and deformed (or thermally or mechanically loaded) objects using the so-called phase stepping method. For both the reference and deformed objects the interference pattern on the camera consists of the superposition of two images with different paths through the interferometer:

1. Path 1 through the reference mirror and
2. Path 2 through the shearing mirror

The displacement vector between both images (in length and direction) is called the shearing vector. Phase stepping is done by varying one of the paths in the interferometer with distances causing phase shifts of $2\pi/n$ with n the number of steps and making a recording (picture) of each step. A minimum of three steps is required to process the data and obtain the phase distribution for both the reference as deformed objects. The phase difference distribution between both objects is a measure for the strain gradient distribution in the direction of the shear vector. Note that the phase stepping images are made at a constant shear vector.

4.1 Phase stepping processing

The phase stepping images at specific load (unloaded or reference or loaded) are built up of the interference pattern of two coherent light beams (where 1 path is varied slightly by moving the mirror (by a typical amount of about 1/10,000 mm, depending on the wavelength of the laser)). If one assumes that signal following path 1 is given by

$$s_1 = A_1 \cos(\omega t + \varphi_1) \text{ [1]}$$

and the signal following path 2 with variable length by

$$s_2 = A_2 \cos(\omega t + \varphi_2 + \varphi_3) \text{ [2]}$$

where φ_3 represents the phase stepping difference $2\pi/n$ (n is number of phase steps; minimum value is 3).
The intensity of the interference pattern is given by

$$\mathrm{I} = \frac{1}{\mathrm{T}}\int [\mathrm{A}_1 \cos(\omega \mathrm{t} + \varphi_1) + \mathrm{A}_2 \cos(\omega \mathrm{t} + \varphi_2 + \varphi_3)]^2 \mathrm{dt} \text{ [3]}$$

$$I = \frac{{A_1}^2}{2} + \frac{{A_2}^2}{2} + A_2 A_1 \cos(\varphi_1 - \varphi_2 - \varphi_3) \text{ [4]}$$

This equation has the same form as the equations from the minimum number of phase stepping equations with φ_3 $2\pi/3$ and unknown function I_0, γ_0 and φ of (x,y):

$$I_1 = I_0[1 + \gamma_0 \cos(\varphi - \tfrac{2\pi}{3})]\ [5]$$

$$I_2 = I_0[1 + \gamma_0 \cos(\varphi)]\ [6]$$

$$I_3 = I_0[1 + \gamma_0 \cos(\varphi + \tfrac{2\pi}{3})]\ [7]$$

From above equations the phase φ can be calculated according to equation

$$\varphi = tan^{-1}[\sqrt{3}\tfrac{(I_3 - I_1)}{(2I_2 - I_1 - I_3)}]\ [8]$$

It is noted that additional and other phase steps may be taken by the displacements of one mirror leading to modified equations.

4.2 Directivity effects and multi-component measurement

The directivity effects caused by various angles of source and detection beams and their influence on the sensitivy for the strain gradient measurement are extensively treated in references [8] [9](see Figure 4).

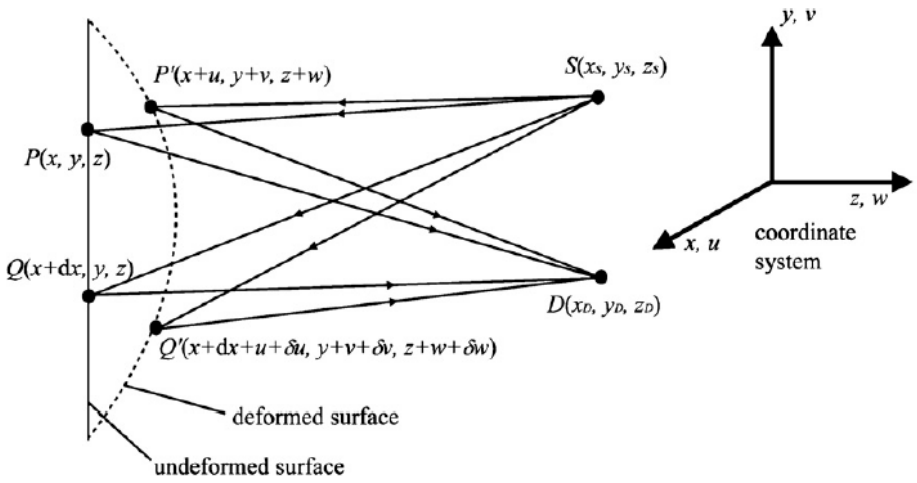

Figure 4: Diagram showing the optical paths between the sources S and detector D for two points on the object's surface, P and Q separated by the shear distance dx, before and after deformation. The coordinate system shows that u, v and w are the displacement components in the x, y and z directions, respectively [8] [9]

The measured phase difference caused by the deformation is given by

$$\Delta\varphi = \tfrac{2\pi}{\lambda}\left[k_x \tfrac{\delta u}{\delta x} + k_y \tfrac{\delta v}{\delta x} + k_z \tfrac{\delta w}{\delta x}\right] dx\ [9]$$

with $k_x = \tfrac{x - x_D}{R_D} + \tfrac{x - x_S}{R_S}$ *[10],* $k_y = \tfrac{y - y}{R_D} + \tfrac{y - y_S}{R_S}$ *[11] and* $k_z = \tfrac{z - z_D}{R_D} + \tfrac{z - z_S}{R_S}$*.[12]*

R_D and R_S are given by the following equations, which differ from those given in references [8] [9]where (x,y,z) is assumed to be (0,0,0):

$$R_D = \sqrt{(x - x_D)^2 + (y - y_D)^2 + (z - z_D)^2}\ [13] \text{ and } R_S = \sqrt{(x - x_S)^2 + (y - y_S)^2 + (z - z_S)^2}\ [14]$$

In case the source and detection beams are collinear (nearly parallel in z-direction leading to k_z=2) the out of plane displacement derivatives are given depending on the directivity of the shear vector by $\frac{\partial w}{\partial x} = \frac{\lambda \Delta \varphi}{4\pi dx}$ [15] and $\frac{\partial w}{\partial y} = \frac{\lambda \Delta \varphi}{4\pi dy}$ [16]. The displacement derivatives in the (x,y) plane follow from these equations by multiplication with the components of an arbitrary unit vector (e_x,e_y) in the (x,y)-plane

$$\frac{\partial w}{\delta \vec{e}} = e_x \frac{\lambda \Delta \varphi_x}{4\pi dx} + e_y \frac{\lambda \Delta \varphi_y}{4\pi dy}\ [17]$$

The above equations hold for the out of plane displacement derivatives. Multi-component measurement requires at least three successive measurements (three sources at different angles and the detection unit (camera) at fixed angle or vice-versa, Figure 5 [8] [9].

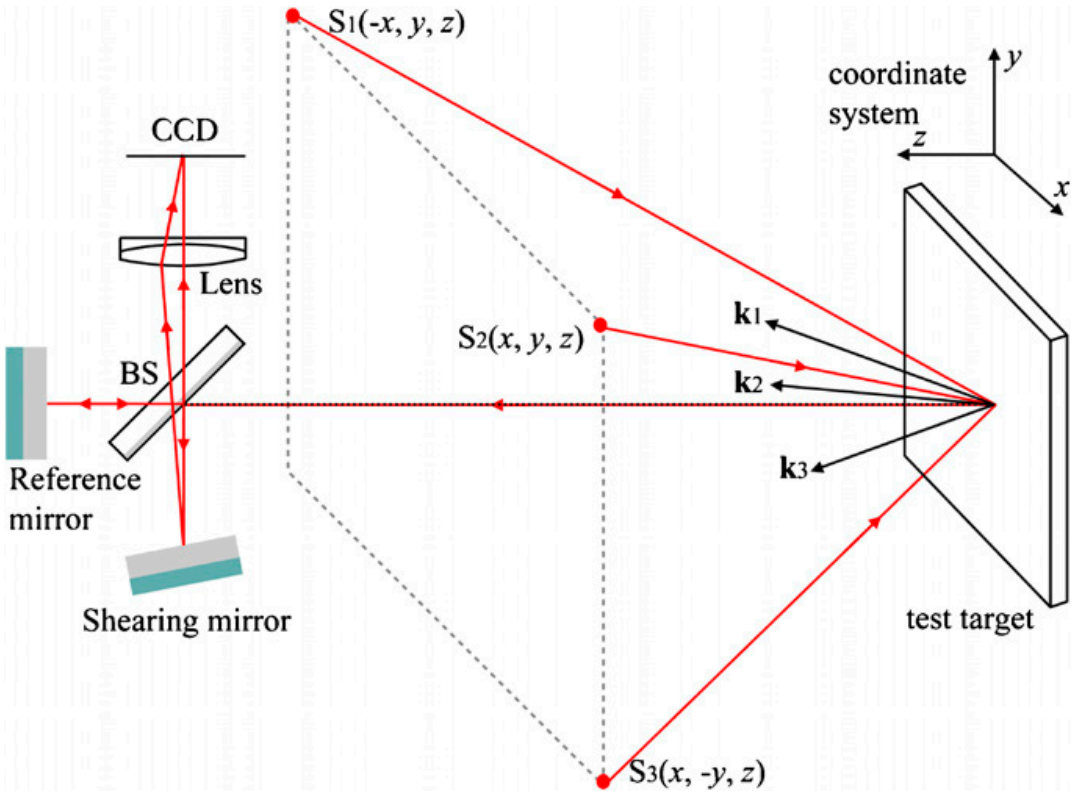

Figure 5: A multi-component shearography system with three sources located at positions S1, S2 and S3. The sensitvity vectors of the measurement channels formed by the three sources are given by k1, k2 and k3

Assuming that the shear vector is in x direction, the optical phase difference measured using each of the illuminating sources is given by

$$\Delta\varphi_{S1} = \frac{2\pi}{\lambda}\left[k_{x1}\frac{\delta u}{\delta x} + k_{y1}\frac{\delta v}{\delta x} + k_{z1}\frac{\delta w}{\delta x}\right] dx\ [18]$$

$$\Delta\varphi_{S2} = \frac{2\pi}{\lambda}\left[k_{x2}\frac{\delta u}{\delta x} + k_{y2}\frac{\delta v}{\delta x} + k_{z2}\frac{\delta w}{\delta x}\right] dx \quad [19]$$

[11b]

$$\Delta\varphi_{31} = \frac{2\pi}{\lambda}\left[k_{13}\frac{\delta u}{\delta x} + k_{y3}\frac{\delta v}{\delta x} + k_{z3}\frac{\delta w}{\delta x}\right] dx \quad [20]$$

The displacement derivatives can be found by matrix inversion of the above equations

$$\begin{pmatrix} \frac{du}{dx} \\ \frac{dv}{dx} \\ \frac{dw}{dx} \end{pmatrix} = \frac{\lambda}{2\pi}\begin{pmatrix} k_{x1} & k_{y1} & k_{z1} \\ k_{x2} & k_{y2} & k_{z2} \\ k_{x3} & k_{y3} & k_{z3} \end{pmatrix}^{-1} \begin{pmatrix} \Delta\varphi_{S1} \\ \Delta\varphi_{S2} \\ \Delta\varphi_{S3} \end{pmatrix} dx^{-1} \quad [21]$$

If one proceeds the same sequence with the shear vector directed in the y-direction the following equation is found

$$\begin{pmatrix} \frac{du}{dy} \\ \frac{dv}{dy} \\ \frac{dw}{dy} \end{pmatrix} = \frac{\lambda}{2\pi}\begin{pmatrix} k_{x1} & k_{y1} & k_{z1} \\ k_{x2} & k_{y2} & k_{z2} \\ k_{x3} & k_{y3} & k_{z3} \end{pmatrix}^{-1} \begin{pmatrix} \Delta\varphi_{S4} \\ \Delta\varphi_{S5} \\ \Delta\varphi_{S6} \end{pmatrix} dy^{-1} \quad [22]$$

If the strain tensor *S* is considered, it follows that only four elements can be fully determined: ε_{xx}, ε_{yy} and $\varepsilon_{xy}=\varepsilon_{yx}$.

$$S = \begin{pmatrix} \varepsilon_{xx} & \varepsilon_{xy} & \varepsilon_{xz} \\ \varepsilon_{yx} & \varepsilon_{yy} & \varepsilon_{yz} \\ \varepsilon_{zx} & \varepsilon_{zy} & \varepsilon_{zz} \end{pmatrix} \quad [23]$$

as shown in the boxed elements in Figure 6

$$= \begin{bmatrix} \boxed{\frac{\partial u}{\partial x}} & \boxed{\frac{1}{2}\left(\frac{\partial u}{\partial y} + \frac{\partial v}{\partial x}\right)} & \frac{1}{2}\left(\frac{\partial u}{\partial z} + \boxed{\frac{\partial w}{\partial x}}\right) \\ \boxed{\frac{1}{2}\left(\frac{\partial v}{\partial x} + \frac{\partial u}{\partial y}\right)} & \boxed{\frac{\partial v}{\partial y}} & \frac{1}{2}\left(\frac{\partial v}{\partial z} + \boxed{\frac{\partial w}{\partial y}}\right) \\ \frac{1}{2}\left(\boxed{\frac{\partial w}{\partial x}} + \frac{\partial u}{\partial z}\right) & \frac{1}{2}\left(\boxed{\frac{\partial w}{\partial y}} + \frac{\partial v}{\partial z}\right) & \frac{\partial w}{\partial z} \end{bmatrix} \quad [24]$$

Figure 6: Boxed elements which can be determined using multi-component shearography measurement (at least 6 measurements are required, [8] [9]

The reason is that the shear vector cannot be directed into the object, which would require a measurement into the volume of the object. This impossibility results into zero displacement derivatives in the z direction (the illuminated object surface is assumed to be parallel to the (x,y)-plane).

The analysis of the multi-component measurement shows the sensitivity of the displacement derivatives on source and detection directions. For most applications the system is optimised for the measurement of out-of-plane displacement derivative by placing the source and camera perpendicular to the surface of the object (collinear set-up).

4.3 Methods of excitation

Using shearography requires the object under inspection to be loaded, to be put under some form of stress.
As mentioned before, the surface of the component will then deflect, causing the length of the laser beam path to change and the speckle pattern to change. The most common methods to stress a component in order to use shearography are:

4.3.1 Thermal excitation

The most versatile in the line of possible excitation methods is thermal excitation. It doesn't require any large hardware investments: often the only thing needed next to a laptop and the shearography camera is a halogen lamp. The setup can be altered fairly quickly and it applies stress in a non-contact way, so it can also be used for large components.
Thermal excitation is also the method used by the NLR and thus for this assignment. The reason for this is the previous research into thermography, where halogen lamps were used for excitation. The most logical thought when thinking ahead to the multi-domain NDT-product would be to use the same method of excitation.
Also, a big advantage of thermal excitation is that it can be used to inspect a component when there is access from one side only. A disadvantage is the (lack of) uniformity of the excitation, because the usage of lamps on larger surface inevitably leads to local overheating relative to the global excitation.

4.3.2 Vacuum excitation

Another way of applying stress to a component is to place it in an airtight environment and subsequently reduce the ambient pressure by sucking the air out (vacuum). This accentuates any internal disbonds or delamination.There are two options in creating the vacuum; one of them is placing the entire component inside of a vacuum chamber. However, the most common system is one with a 'vacuum hood', where a small suction chamber is created by placing a rigid frame with Perspex window equipped with rubber strips on the surface of the component. The shearography equipment can then perform measurements through the Perspex window.
While vacuum excitation when using a vacuum hood is a very suitable method for shearography, because of its ability to apply a uniform stress, it is limited by the size of the hood and is incapable of inspecting complex shapes. These limitations do not apply when placing the whole component inside of a vacuum chamber, but this requires the component to be removed from the potential assembly. [10]

4.3.3 Vibration excitation

By introducing elastic waves into solid materials, surface deformations periodically arise. Defects like delamination will usually vibrate with a higher frequency in respect to the frequency of the component. These differences in frequency result in thermal energy, caused by friction, which subsequently leads to surface displacement that can be measured by the shearography equipment.
Vibration as a form of excitation is especially effective when inspecting materials with a higher stiffness, like ceramics for instance.

5 Edevis equipment and processing

5.1 Description of NLR Edevis shearography equipment

The Edevis shearography setup consists of a few elements, which will be briefly explained hereafter:

1. Two halogen excitation lamps,
2. A varying number of laser diodes (additional laser diodes were rented from Edevis to enlarge the field of view),
3. Isi-sys SE 2 camera and
4. A pc with Edevis shearovis software.

Relevant specifications of the used equipment are listed in Appendix A.

5.1.1 Shearography camera

The shearography camera (Isi-sys SE 2) is equipped with a Sigma ED camera lens (Figure 7). The interferometer set-up with beam splitter, reference and shearing mirrors are integrated. The maximum frame rate of the camera is 15 Hz at a reduced resolution of 1226x1028 pixels.

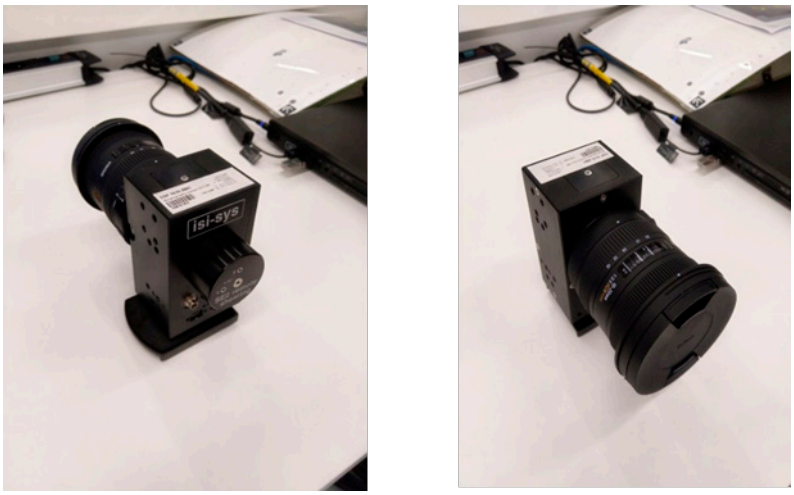

Figure 7: Edevis Isi-Sys SE 2 camera

5.1.2 Diode-laser arrays

Since shearography is a method of laser speckle interferometry, the lasers are indispensable. Made by the same manufacturer, the diode laser arrays consist of five diodes each, as can be seen in Figure 8. Each diode has an output of 100 mW. The first tests in the practical part of this research are performed with two laser arrays, while the later tests on larger surfaces include four arrays (Figure 10).

Figure 8: Isi-sys diode laser group (5 units)

5.1.3 Camera setup

On the first setup, the lasers were attached aside to the camera housing. Two groups of diode lasers were rented from Edevis and additional support struts were added to the camera to mount the four laser groups (Figure 10). To improve the mobility of the arrays in the second setup (with four arrays), special hydraulic support arms were used, which can be seen in Figure 9.

Figure 9: Hydraulic support arms for additional laser groups

It is noted that in the final set-up the camera and the laser diodes are not perfectly aligned given rise to some uncertainty or error in the measurement of out-of-plane displacement gradients.

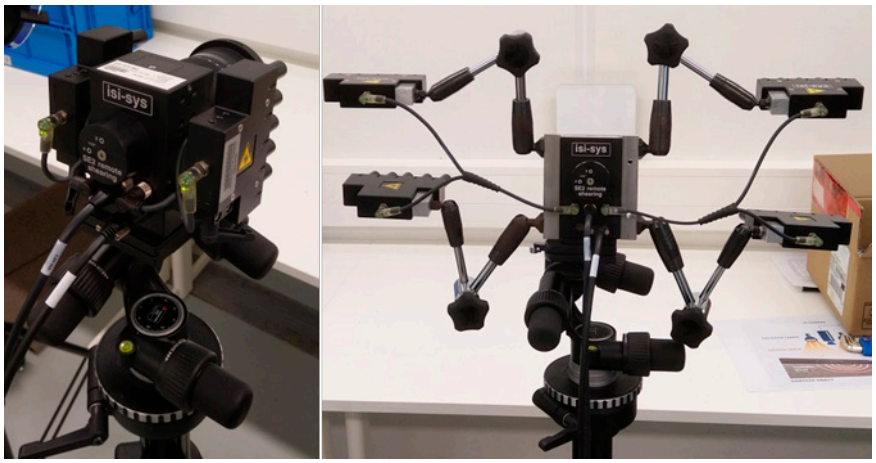

Figure 10: The first camera setup (L) and the second setup with four laser arrays (R)

5.1.4 Halogen excitation lamp

Finally, the excitation is provided by two Hedler lights that can be seen in Figure 11. The lights both have an output of 2000 W, with a total system power of 4000 W.

Figure 11: Two Hedler lamps used for thermal excitation

5.2 Edevis shearography processing

Thermal loading on the object is applied to obtain the required deformations. Edevis uses a five stepping phase (also called Carré, [11] [12]) algorithm with phase steps ranging –π/2 to π/2 (instead of -π to π) to obtain $\varphi(x, y)$ with a least-squares method.

$$tan(\varphi) = \frac{\sqrt{4(I_2 - I_4)^2 - (I_1 - I_5)^2}}{2I_3 - I_1 - I_5} \text{ [25]}$$

A measurement sequence consists of four steps (Figure 12-Figure 14]:

1. Take 5 images at fixed shear vector and varying optical path (shearing mirror) of the reference and deformed object.
2. Calculate for phase distribution φ, using the 5 images.
3. Subtract the phase distributions found for the reference and deformed object to obtain the so-called wrapped phase image of $\Delta\varphi$ ($-\pi < \varphi < \pi$) and
4. Unwrap the phase image.

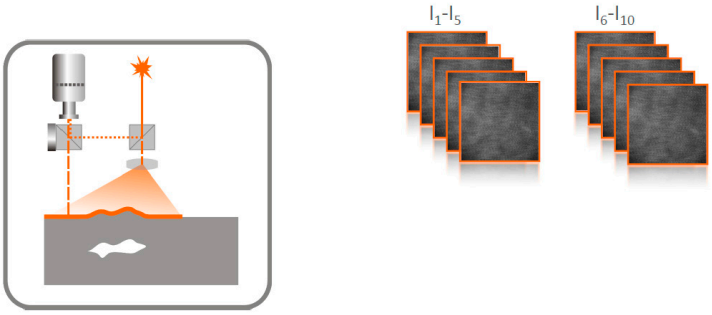

Figure 12: Step 1 taking the images [12]

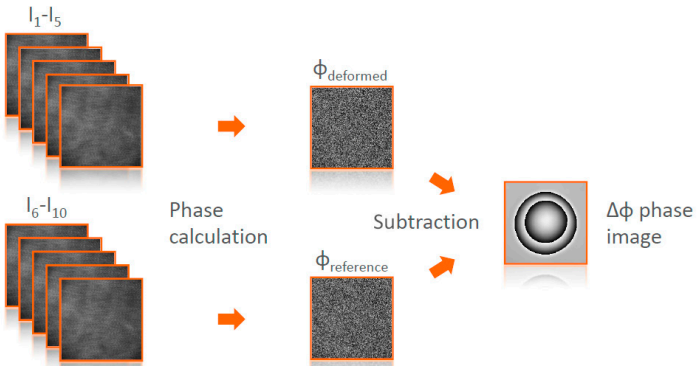

Figure 13: Step 2 calculating the phase distributions (ref. Edevis)

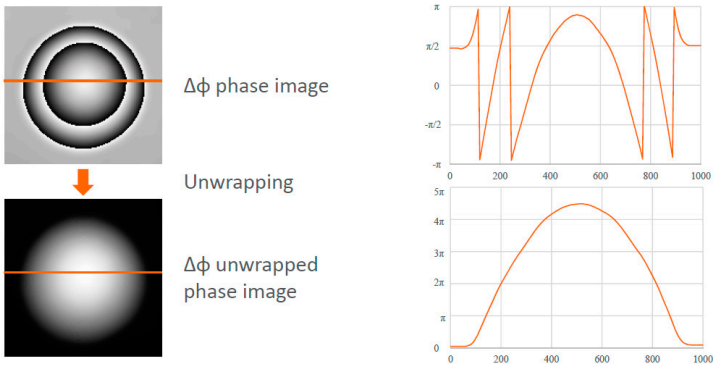

Figure 14: Steps 3 & 4. Subtract the phase distributions to obtain the wrapped phase difference distribution and unwrap the phase [12]

Edevis equipment offers also the possibility to make time series with alternating phase to obtain ΔI-plots (Intensity) between successive images. This feature can help to select the optimal time frame for making the Δφ-images.

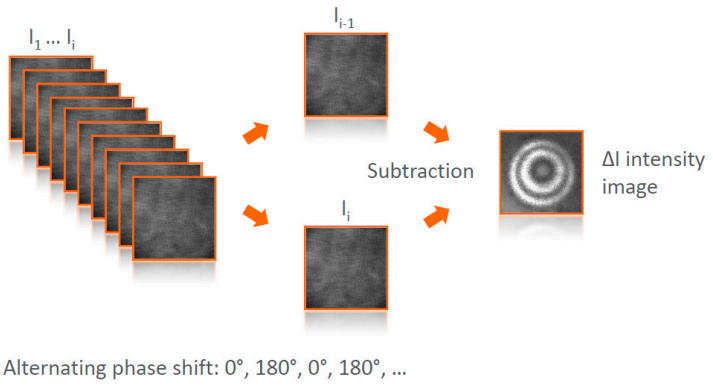

Figure 14: Time series on successive intensity images with alternating phase [12]

6 Test samples

This chapter states the test samples used in the research. The first test sample is a standard calibration sample used for shearography. The focus in de DCMC project is on composite structures, so two composite test samples are selected for the generation of first impressions and results. Test sample used in this study are:

1. Edevis shearography calibration sample.
2. A generic monolithic composite test sample containing inserts and impact damage (also known as NLR-A2).
3. A generic composite test sample with sandwich structure and a core of Nomex honeycomb (also known as NLR-C).

6.1 Edevis shearography calibration sample

The aluminium test component (approx. 20x20x2 cm) is provided by the manufacturer with the intention to be able to perform demonstrations to potential clients. To do this, multiple excitation possibilities are included in the component, such as the piezo-element that is stuck on the back side of the component (Figure 15), which makes it possible to perform measurements using vibration as an excitation method. The deformation is applied in a quite simple manner: the beam on the back side has an Allen screw in the middle (designated by the red circle). As the screw is tightened, the front side of the component is slightly deformed, resulting in a clear circle on the shearogram.

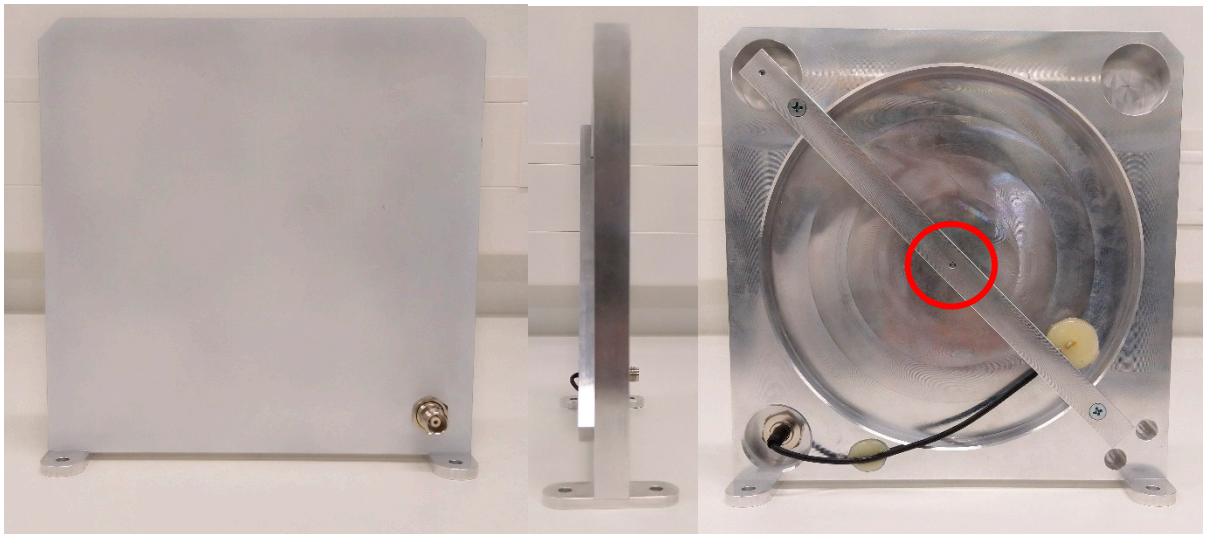

Figure 15: Aluminium test component (left) Front-side (right) back side

6.2 Generic composite panel 1 (NLR-A2)

Specimen NLR-A2 is a solid laminate with dimensions of 900 x 600 mm. The thickness of specimen NLR-A2 is overall 5.4 mm. The laminate consists of 24 layers with quasi-isotropic lay-up. Half of the specimen is covered with a copper wire mesh, simulating the lightning protection. For an overview of the specimen, see Figure 16. Both parts of the specimen (with/without cupper mesh) contain the following internal defects:

- Interply delaminations, simulated by Teflon foils of diameter 0.25, 0.5 and 1 inch, and placed at three different depths (0.7, 3.4 and 4.7 mm).
- Natural delaminations, caused by impacts with different energy levels and tub diameters. Ultrasonic C-scan data gives information about the appearance and size of the delaminated areas, see Figure 17.

For orientation purposes, adhesive stickers are applied with a diameter of 8 mm both on the top and bottom side and hole D with a diameter of 8 mm.

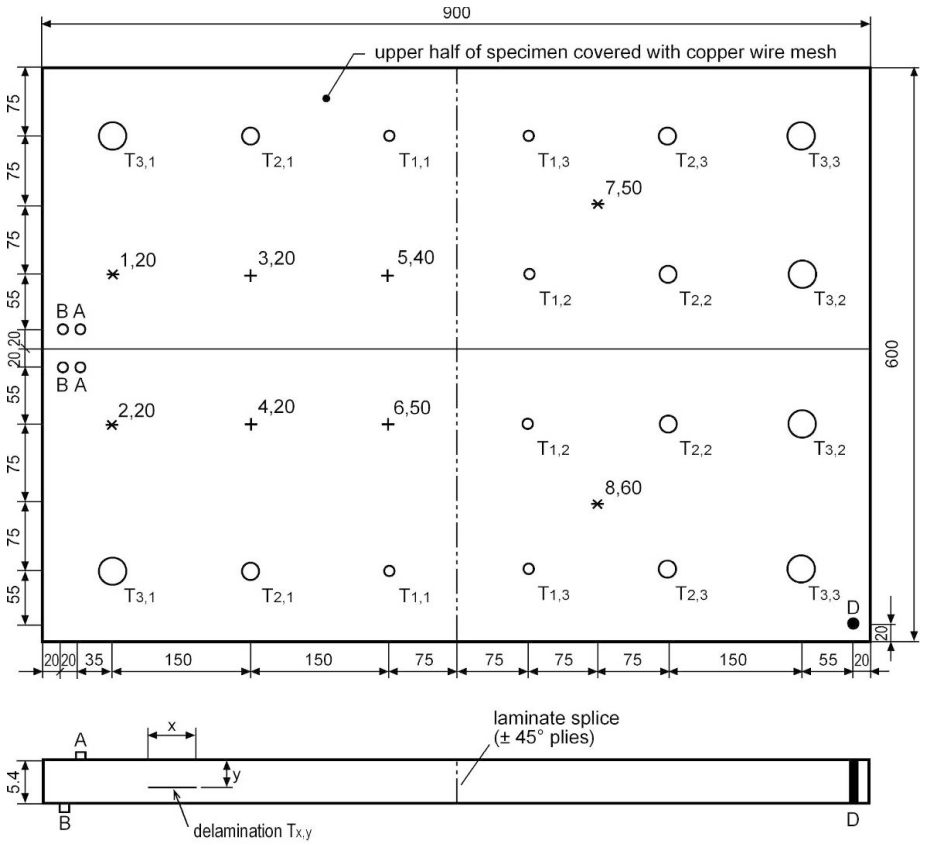

Defect type	
Delamination $T_{x,y}$	x = 1, 2 or 3 Diameter 0.25; 0.5 or 1.0 inch y = 1, 2 or 3 Depth 0.7; 3.4 or 4.7 mm
Impact $+^{x,y}$ $*^{x,y}$	+ / ∗ Impactor tup diameter 0.5/1.0 inch x = Impact number; y = Impact energy [J]
Adhesive sticker	A ∅ 8 mm on top side of laminate B ∅ 8 mm on bottom side of laminate
Hole D	∅ 8 mm

Figure 16: Specimen NLR-A2, structural details solid laminate thickness 5.4 mm

To determine the size of the impact damage an ultrasonic pulse-echo measurement is made, the C-scan test results can be seen in Figure 17 including the width and height dimensions.

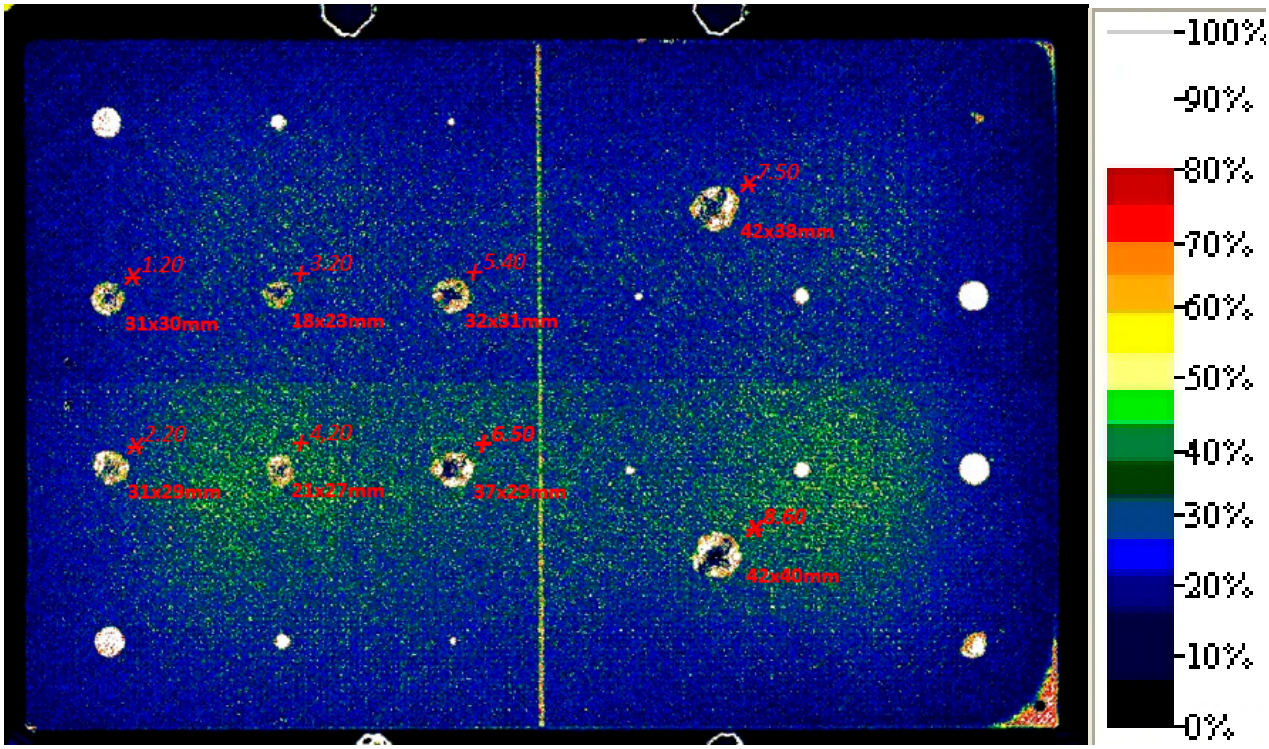

Figure 17: Specimen A2, ultrasonic pulse-echo reflection data (gate between front and backwall reflection) of the impact locations

6.3 Generic composite panel 2 (NLR-C)

Specimen NLR-C is a sandwich structure with dimensions of 900 x 600 mm. The core consists of a Nomex honeycomb with thickness of 19 mm and cell size of 0.25 inch (6.4 mm). The outer and inner skins thickness are 3.0 and 1.5 mm respectively. The outer skin laminate is 12 layers with quasi-isotropic lay-up. The inner skin laminate is 6 layers with quasi-isotropic lay-up. Half of the outer skin laminate is covered with a copper wire mesh. For an overview of the specimen, see Figure 18. Both parts of the specimen (with/without copper mesh) contain the following internal defects:

- Interply delaminations in the outer skin simulated by Teflon foils of diameter 0.25, 0.5 and 1 inch, and placed at two different through-the-thickness positions (depths of 1.5 and 2.25 mm);
- Outer skin-to-honeycomb core disbonds simulated by flat-bottomed holes in the Nomex core of diameter: 0.25, 0.5, 1 and 2 inch;
- Natural delaminations caused by impacts with different energy levels and tub diameters. Ultrasonic data gives information about the appearance and size of the delaminated areas;
- Water ingress in the Nomex honeycomb cells.

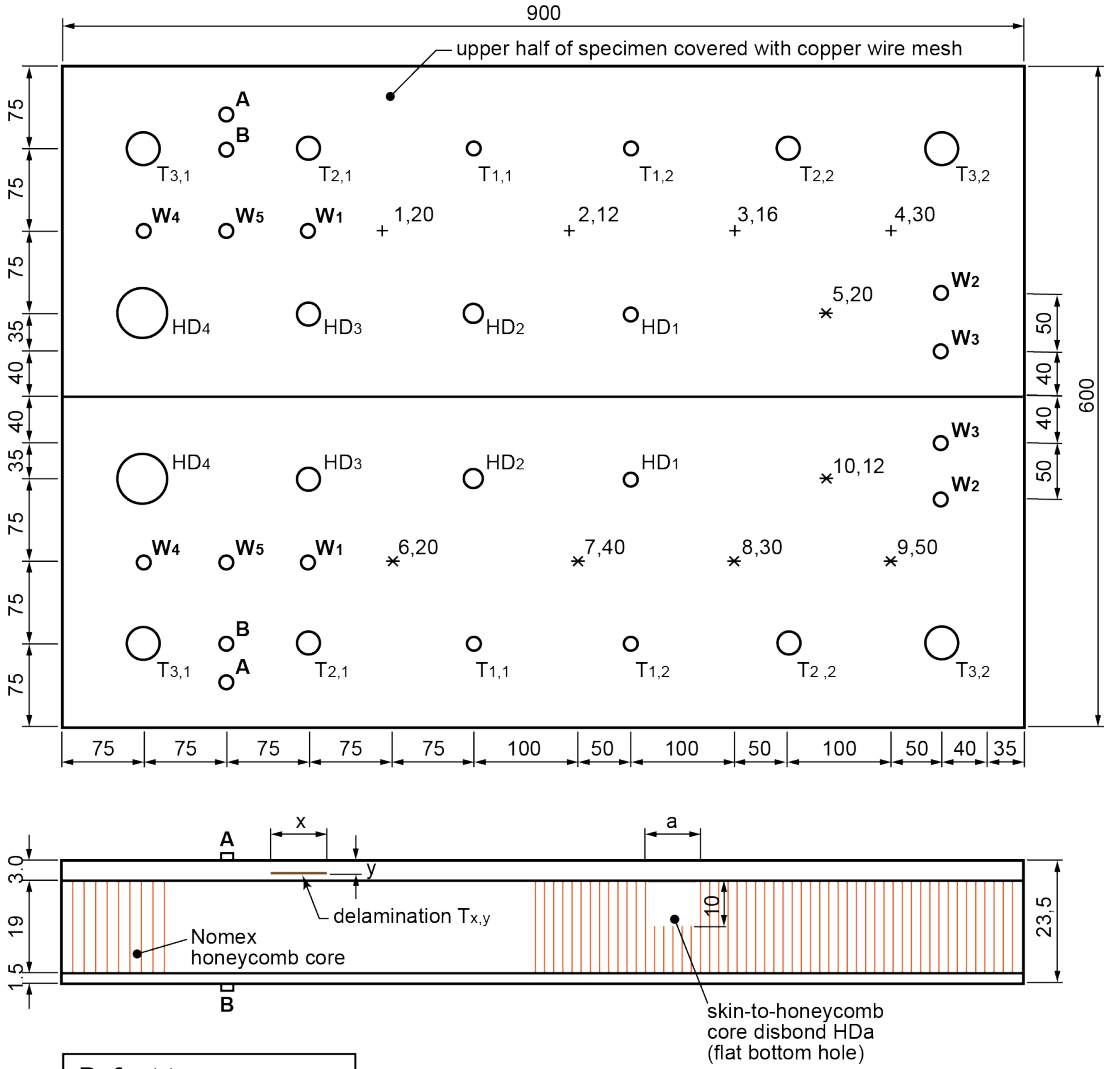

Defect type		
Delamination $T_{x,y}$	x = 1, 2 or 3 y = 1 or 2	Diameter 0.25; 0.5 or 1.0 inch Depth 1.5 or 2.25 mm
Skin-to-honeycomb core disbond HDa	a = 1, 2, 3 or 4	Diameter 0.25; 0.5; 1.0 or 2.0 inch
Impact $+^{x,y}$ $*^{x,y}$	+/* Impactor tup diameter 0.5/1.0 inch x = Impact number; y = Impact energy [J]	
Adhesive sticker	A ∅12 mm on outer skin B ∅12 mm on inner skin	
Water ingress Wx in honeycomb cells (HC)	x = 1 1 HC full x = 2 3 HC full x = 3 3 HC half-full x = 4 7 HC full x = 5 7 HC half-full	

Figure 18: Specimen NLR-C, structural details sandwich structure

To determine the size of the impact damage in the skin, an ultrasonic pulse-echo measurement is performed. The C-scan test results can be seen in Figure 19, including the width and height dimensions of the damages.

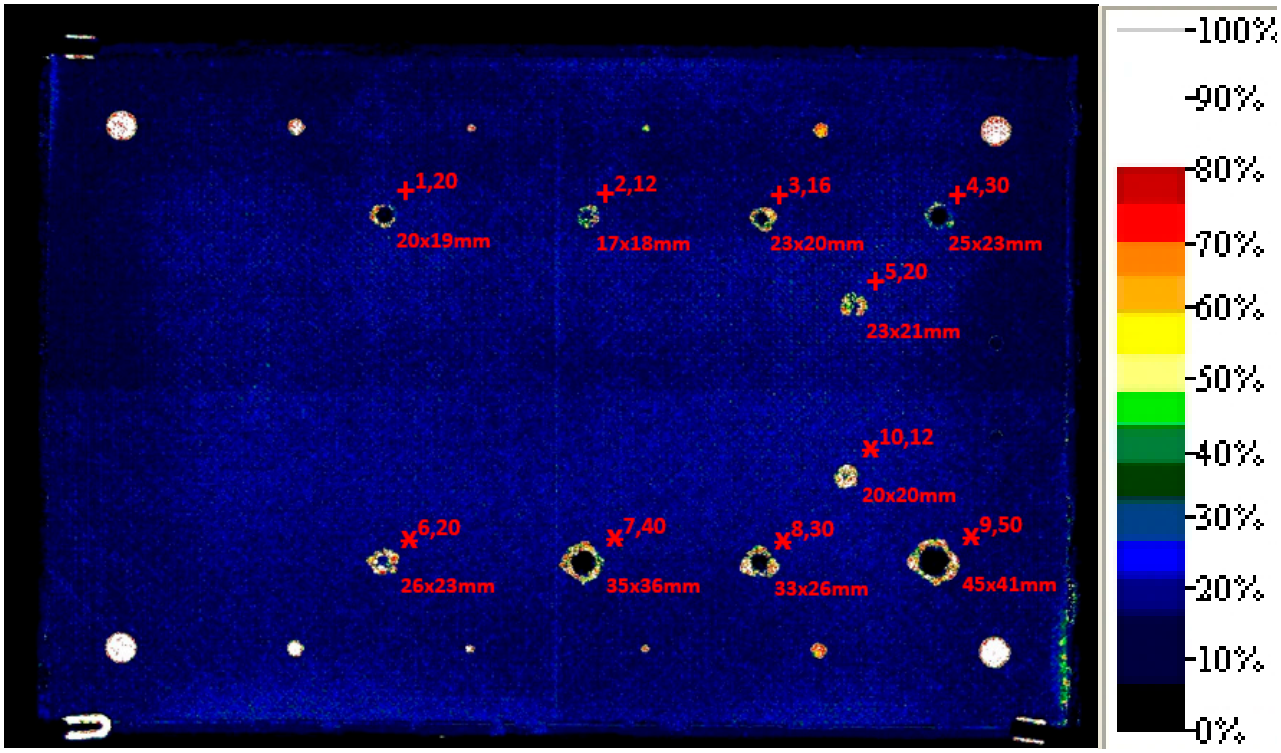

Figure 19: Specimen NLR- C, ultrasonic pulse-echo data reflection of the impact damage locations

Next to the delamination damage in the skin, also a skin-to-core disbond can occur. This type of damage can only be detected with the ultrasonic through-transmission technique, for which two sided access is needed. The size of the skin-to-core disbond can be seen in Figure 20. On the other hand, the through-transmission C-scan data does not shows a complete attenuation of the sound beam at the impact location. This is an indication that the core is not completely separated from the skin.

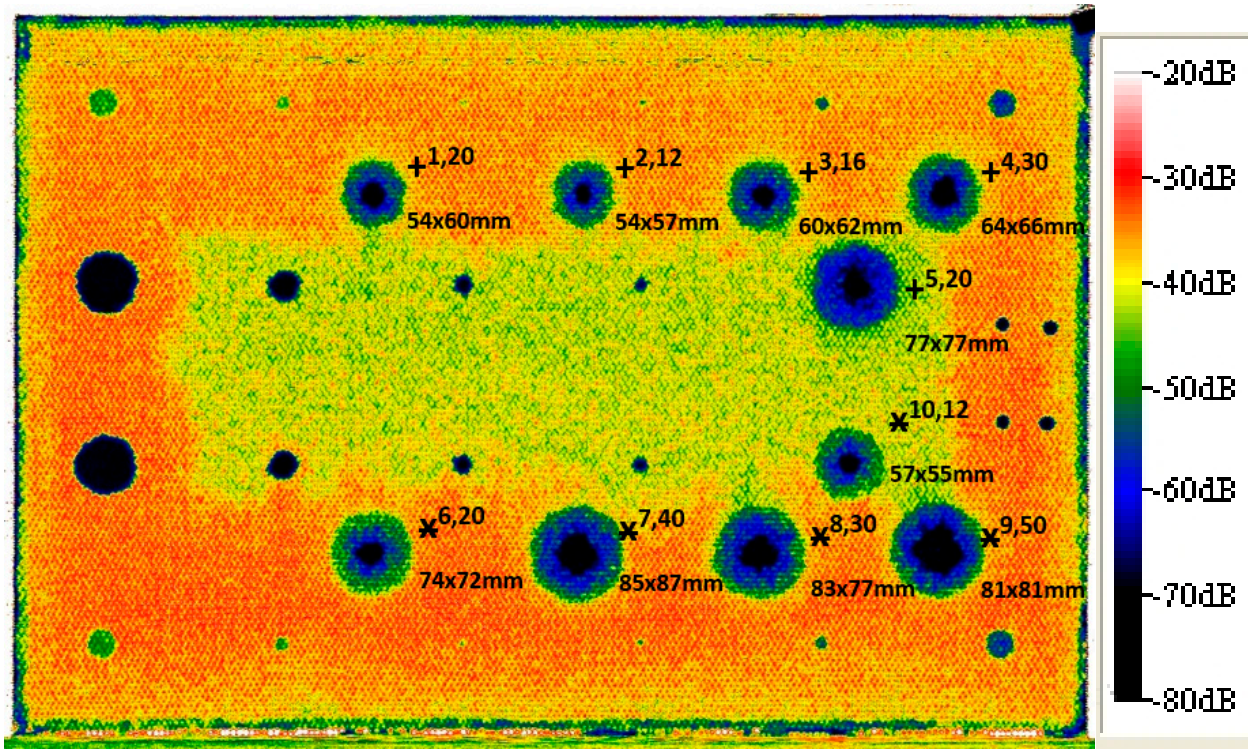

Figure 20: Specimen NLR-C, ultrasonic through-transmission data of the impact damage locations

7 Results and discussion

This chapter analyses the results gathered during the internship of Rik Lambrichs(InHolland University of Applied Sciences Delft), [4] on the calibration sample. Further, NLR performed experiments on the two composite panels, the shearography test results will be reported and discussed.

7.1 Edevis calibration sample

The practical tests in this research started off by researching the various parameters that appear from the theory. In the first test phase, the focus was primarily laid on the software, starting with the frame rate in combination with the integration time. These two factors are linked to each other. The integration time can be compared to the shutter speed of the average camera, which summarises to the fact that a dark surface requires a higher integration time and a light surface a lower integration time.

The first series of tests is performed on the aluminium test component, as described in the previous chapter. The first topic is the integration time and its effect. The integration time parameter has a direct influence on the intensity (dL) which is, concluding from the theory in section 2.2.1 (section on interference), a variable that should ideally be around 4065 dL (difference in digital level; unit for intensity) in the measurements. The following default settings were used during the integration time tests using 2 laser arrays (Figure 21).

Excitation amplitude: 75%

Pulse length: 5s.

Timing of reference image: 0s.

Timing of displacement image: 7s

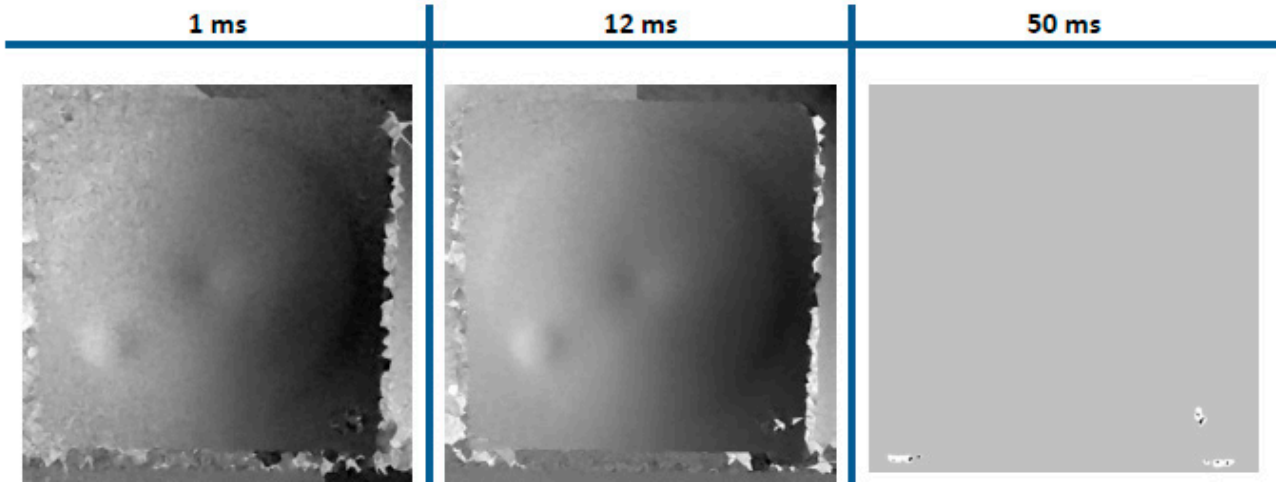

Figure 21: Effect of varying integration time on Edevis calibration sample

The out-of-plane displacement can be seen in the images as the big large circle. The small circle is the piezo element that is attached to the panels as can be seen in Figure 15. As can be seen in the results above, the image starts to get 'granular' as the integration time goes down. An integration time of 12 ms provides the best result, while a relatively high integration time of 50 ms gives an overexposed result. This object does have an ideal surface in terms of reflection (white and matte).
A less ideal surface could require a higher integration time depending on the reflectiveness and colour of the component. However, the results above show the general effect of varying the integration time. If the surface has a different colour the integration time must be adjusted such that the DL values are in the correct range. For black composite material these integration times will be orders higher as compared to calibration sample.
The following results emerge when subsequently perform measurements using a frame rate of 1 Hz, 5 Hz, 8 Hz and 12 Hz (Figure 22). Note that the shearography camera has a maximum frame rate of 15 Hz as described in the chapter on the methodology. Furthermore, the same settings were used as during the tests on the integration time, using a fixed integration time of 15 ms.

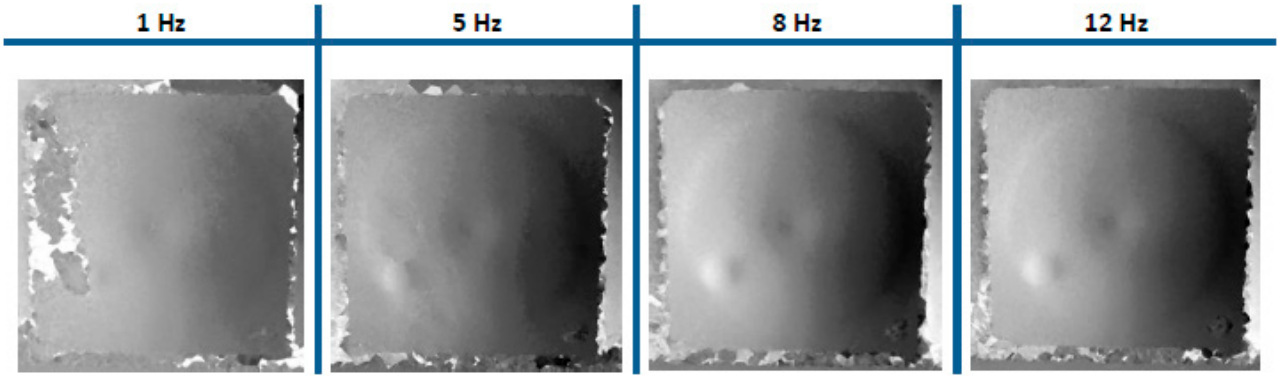

Figure 22: Effect of varying frame rate on Edevis calibration sample

From these images, the conclusion is derived that the frame rate is not a decisive variable in obtaining a result, but that the integration time set is leading. As the framerate increases the five intensity images that are used for the phase images are taken at a shorter timeframe, making them less susceptible for vibrations.

One thing that immediately shows up during these initial tests is the logical requirement to allow the surface under inspection time to cool down between two measurements. When performing measurements quickly one after the other, the reference image, just like the displacement images, will be taken at a time when the object is already deformed. Depending on the material properties of the component under inspection, rapid successive inspections will emerge in no reliable results, because the difference between the local and global displacement is not large enough.

Continuing with the parameters revolving around the software, the excitation pulse length was investigated in addition to the integration time. This is an important factor in this setup, especially with the use of optical excitation using lamps, results are available in [4].

Subsequently, the variables around the hardware are tested, starting with the position of the lamps in relation to the component [4]. However, the sensitivity to vibrations is an issue during these tests. The search for setup where the lamps can easily be moved, led to a long series of tests with no good result. The cause of this appears to be vibrations, caused by the unstable position of the component under inspection. This is confirmed during the tests by placing the component on different supports. The shearogram clearly show the object, but the component itself is covered in noise, as shown in Figure 23.

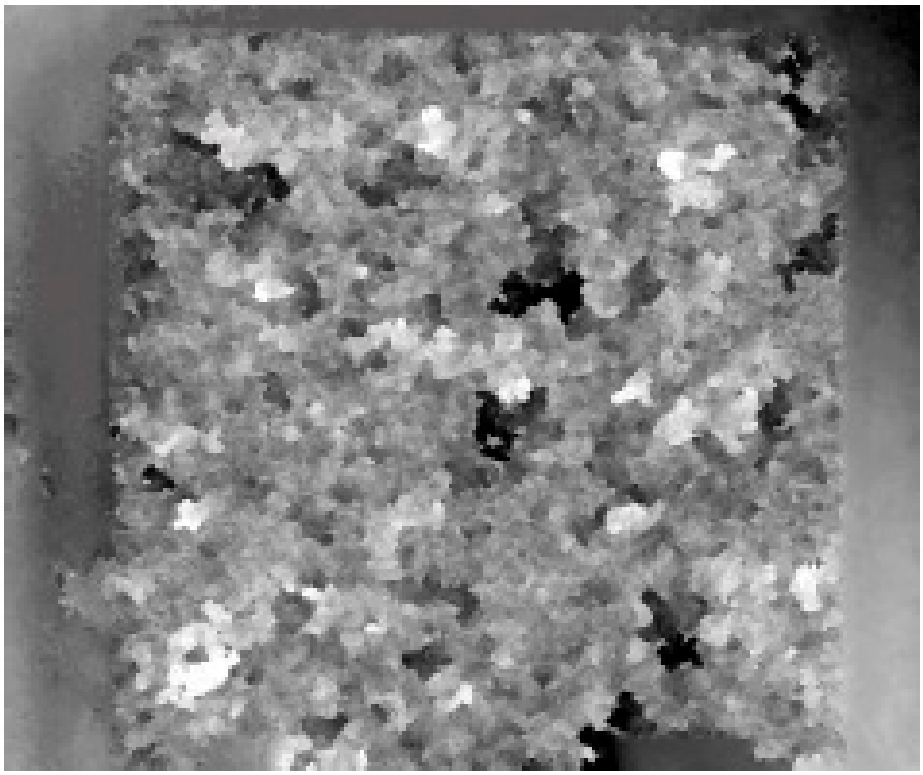

Figure 23: Disturbed results on the calibration sample due to vibrations in the environment

Concluding from the series of tests on the aluminium test panel, the following observations can be stated:

1. When using shearography, it is important to find the optimal settings for the surface under investigation in order to get useful results. It is recommended to set a minimum integration time, keeping the ideal intensity (4065 dL) in mind, enabling the camera to use a maximum frame rate.
2. The high sensitivity to deformations requires a relatively stable setup for the component, preventing distortion caused by excessive external vibrations.
3. In between measurements, it is important to allow a component under inspection to cool down. This is however dependant on the thermal properties of the component.

7.2 Generic composite panel NLR-A2

Shearography inspection has been performed on panel NLR-A2 with the entire panel in the FOV, using four laser arrays. The following parameters were varied for experiments:

- Shear vector (both direction and magnitude)
- Pulse length
- Background image
- Evaluation image

The following parameters were kept constant to reduce the number of parameters:

- Framerate 2.85 Hz
- Integration time 350 ms
- Amplitude 95%
- Position of camera fixed

Due to the green colour of the panel the integration time is roughly ten times as high as for the calibration sample. From the initial experiments on the aluminium calibration sample these parameters had not a major influence on the results as long as they have been set correctly. Figure 24 shows 6 wrapped shearograms of panel NLR-A2 at a shear vector of 9.9 mm at 90^{o} (vertical shear). The pulse length is varied between measurements and indicated in the top right corner of each while the amplitude of the lamps is set at 95%. Both the framerate and integration time are fixed to 2.85Hz and 350 ms, respectively. The reference image is set at frame 171(60 s) and the evaluation at frame 1 (0 s) for all images. The entire panel is captured in a single FOV resulting in a resolution of 0.38 mm/pixel.

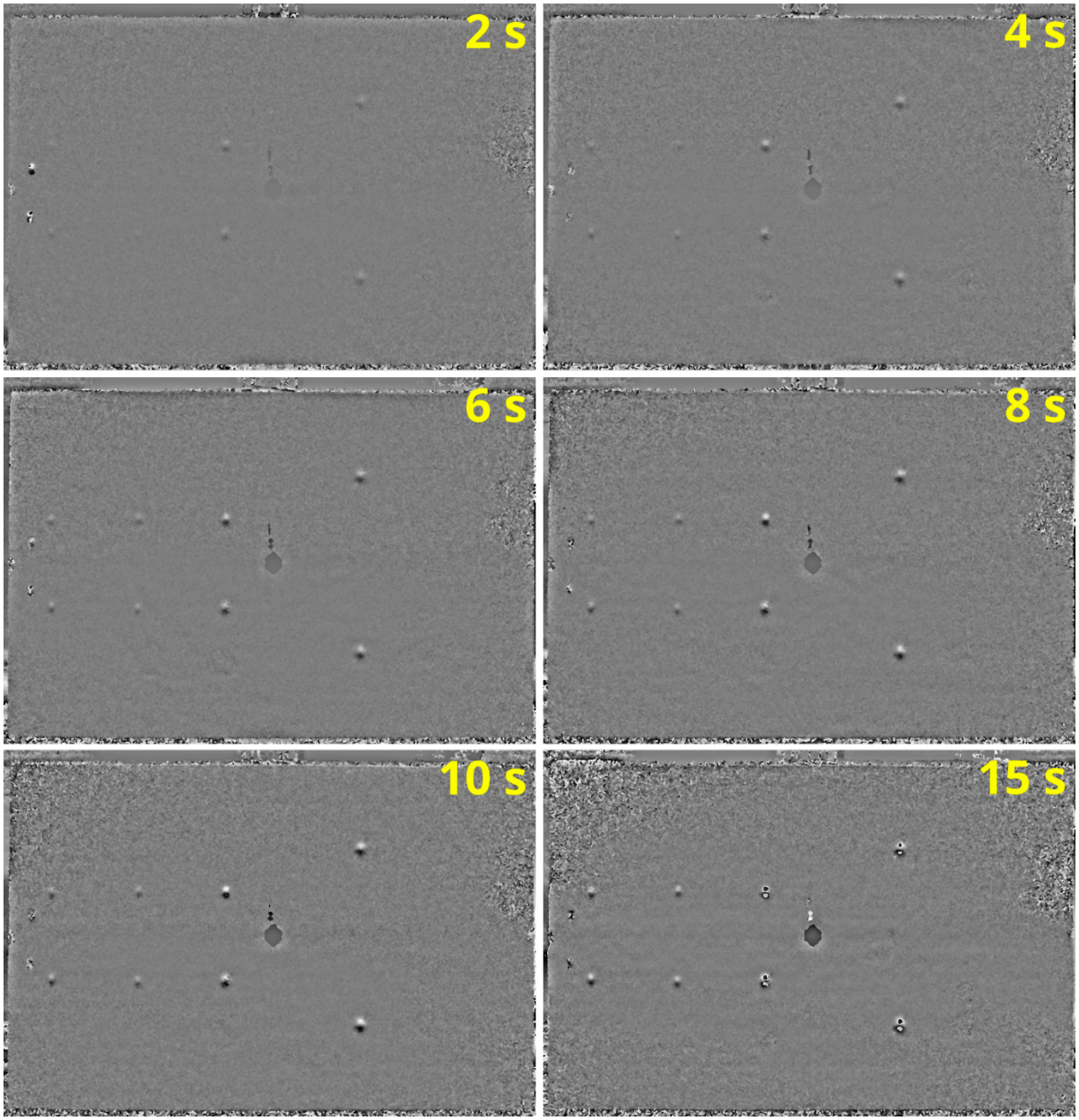

Figure 24: Wrapped shearograms of panel NLR-A2 with a shear vector of 9.9 mm at 90^{o}, the pulse length is varied between images and indicated in the top right corner

By increasing the pulse length of the lamps the sample is heated more, leading to a stronger defect response. At a pulse length of 2 seconds four to six impact locations are visible. By increasing the pulse length to 4 seconds more impact locations can be seen and the contrast is increased. Contrast is the highest for the 15 second pulse length

where clear fringes from four of the eight impact locations can be seen. The corners of the panel start to show decorrelation effects due to the high heat input. Figure 25 shows an overview of the results on the detectability of the artificial defects present in panel NLR-A2.

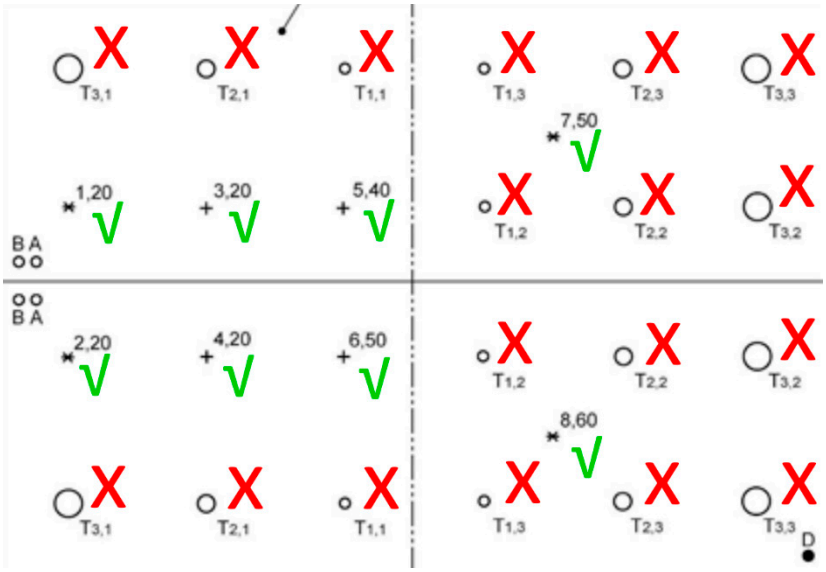

Figure 25: Results of panel NLR-A2. Natural impact damage with a green check mark can be found using shearography. Artificial defects (foil inserts) with a red cross cannot be found with shearography

All impact locations can be found using shearography, also seen in Figure 24. None of the Teflon inserts, simulating a delamination can be found using shearography. The Teflon inserts are a good way to simulate a delamination for the ultrasonic technique, however they do not simulate a delamination for shearography. The Teflon inserts are adhered to the CFRP fibres which means that they transport mechanical load. Using optical excitation, and the corresponding thermal stress that is applied on the surface, does not results in more out-of-plane deviation for areas containing inserts and areas that are free of defects. This makes it impossible to find these inserts. If the defects would be a natural delamination this would result in different mechanical properties which would enable shearography to detect them.

7.3 Generic composite panel NLR-C

The second series of tests is performed on a generic composite panel also described in Section 6.3 on the test samples. The left middle section of the panel contains disbonds, while the surrounding area of the panel contains impact damage and delamination (Figure 18).

The following parameters are varied for the experiments:

- Pulse length (1-15s)
- Shear vector, both in direction and magnitude.
- Evaluation image

The majority of settings were set constant:

- Framerate 2.85 Hz
- Integration time 350 ms
- Amplitude 95%
- Position of camera fixed
- Background image (172)

The panel has the same size, and surface finish (green coating) resulting in same values for integration time and framerate as for panel NLR-A2.

Figure 26 shows the wrapped shearograms of panel NLR-C with different pulse lengths. The vertical shear vector is constant between the images and set to 12.4 mm vertical. The pulse length is indicated in the top right corner of each shearogram. A total record time of 60 seconds is used and the background image is set at 60 seconds. The evaluation image between the shearographs are different due to the difference in pulse length. The shearogram with best defect detectability is selected and shown. At a pulse length of 2 seconds four impact locations show an indication. By increasing the pulse length the amount of out-of-plane deviation is increased and more impact locations become visible at pulse length of 3 seconds (7 out of 10). At a pulse length of 4 seconds all 10 impact locations are visible and four of eight skin-to-core disbonds become visible. Increasing the pulse length even more results in more contrast and smaller skin-to-core disbonds to become visible. At a pulse length of 10 seconds all skin-to-core disbonds are visible and visibility is increased at 15 seconds pulse length.

The combination of the shear magnitude and the gradient of the out-of-plane deviation determine the number of fringes that can be seen on the surface. In order to check this sensitivity the pulse length is kept at 15 seconds, but the shear vector is changed. Figure 27 shows wrapped shearograms of panel NLR-C with different shear vectors, keeping the pulse length constant (15 s). The evaluation image (frame 21, t=7.36s) and the background image (frame 172, t=60s) were set the same for all pictures. The left column of the figure contains shearograms with a horizontal shear (indicated by the yellow arrow) and the right column of the figure contains shearograms with a vertical shear. From top to bottom the shear magnitude is increased starting at 4.4 mm until 12.4 mm. For the most top left image the shearogram shown has a pulse length of 7 seconds instead of 15 seconds. The experiment with a pulse length of 15 seconds was not performed for this shear vector. However, the picture is included such that all shear vectors are shown. Overall, for both shear directions the contrast between sound material and defect increases with an increase in shear magnitude. At the smallest shear magnitude of 4.4 mm all impact locations are visible for the vertical shear. For the horizontal shear this is not the case, but the pulse length was also lower. Additionally, 6 of the 8 skin-to-core disbonds can be detected in the shearogram of the vertical shear. By increasing the shear magnitude, all impacts locations show a higher contrast From 6.7 mm and onward all skin-to-core disbonds can be detected, with more detail/contrast for increasing shear magnitude. The indications for the defects are slightly better visible in the vertical shear direction as in the horizontal shear direction.

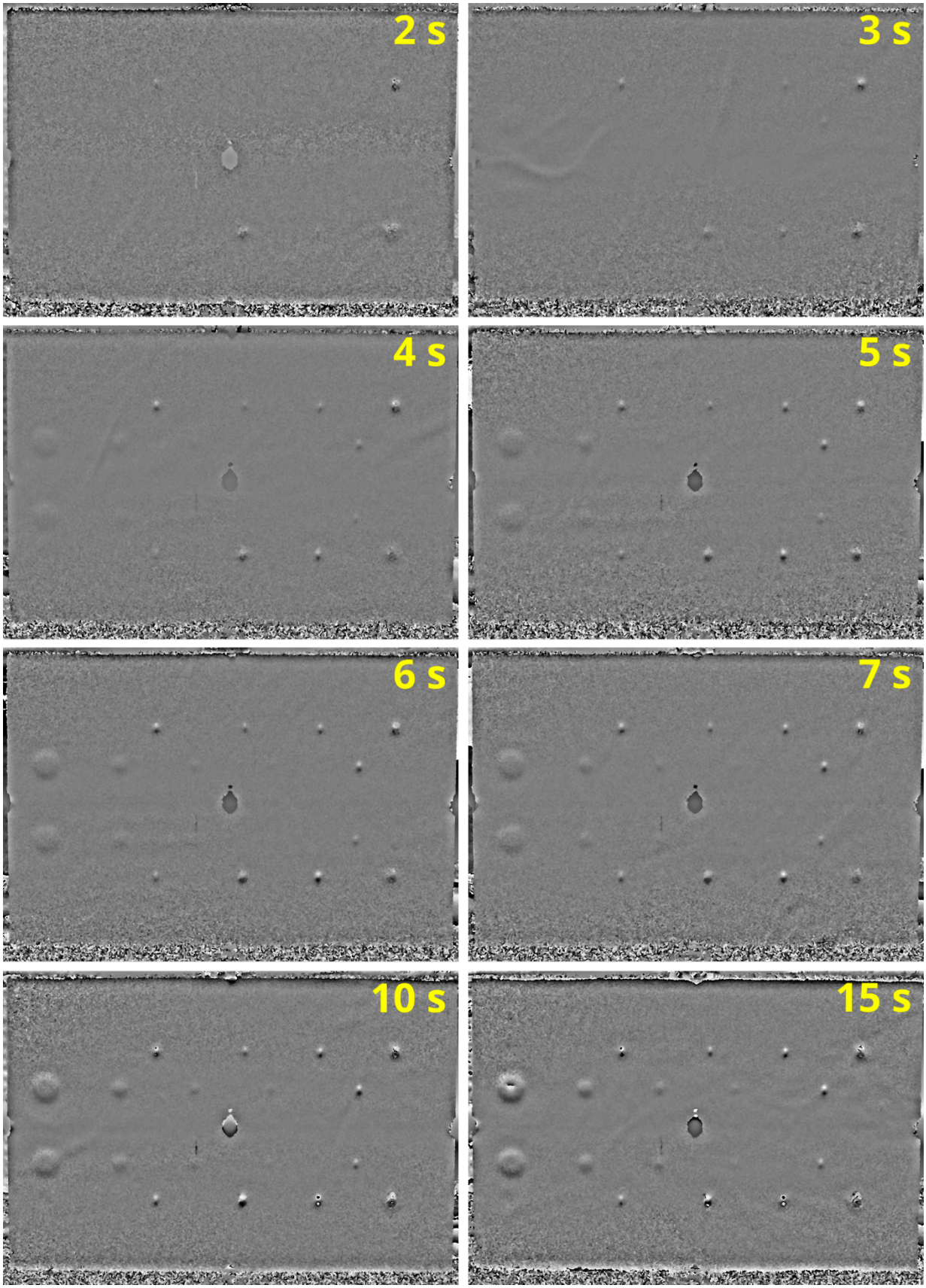

Figure 26: Wrapped shearograms of panel NLR-C with a vertical shear vector with a magnitude of 12.4 mm. The pulse length is varied between the images and stated in the top right corner of each image

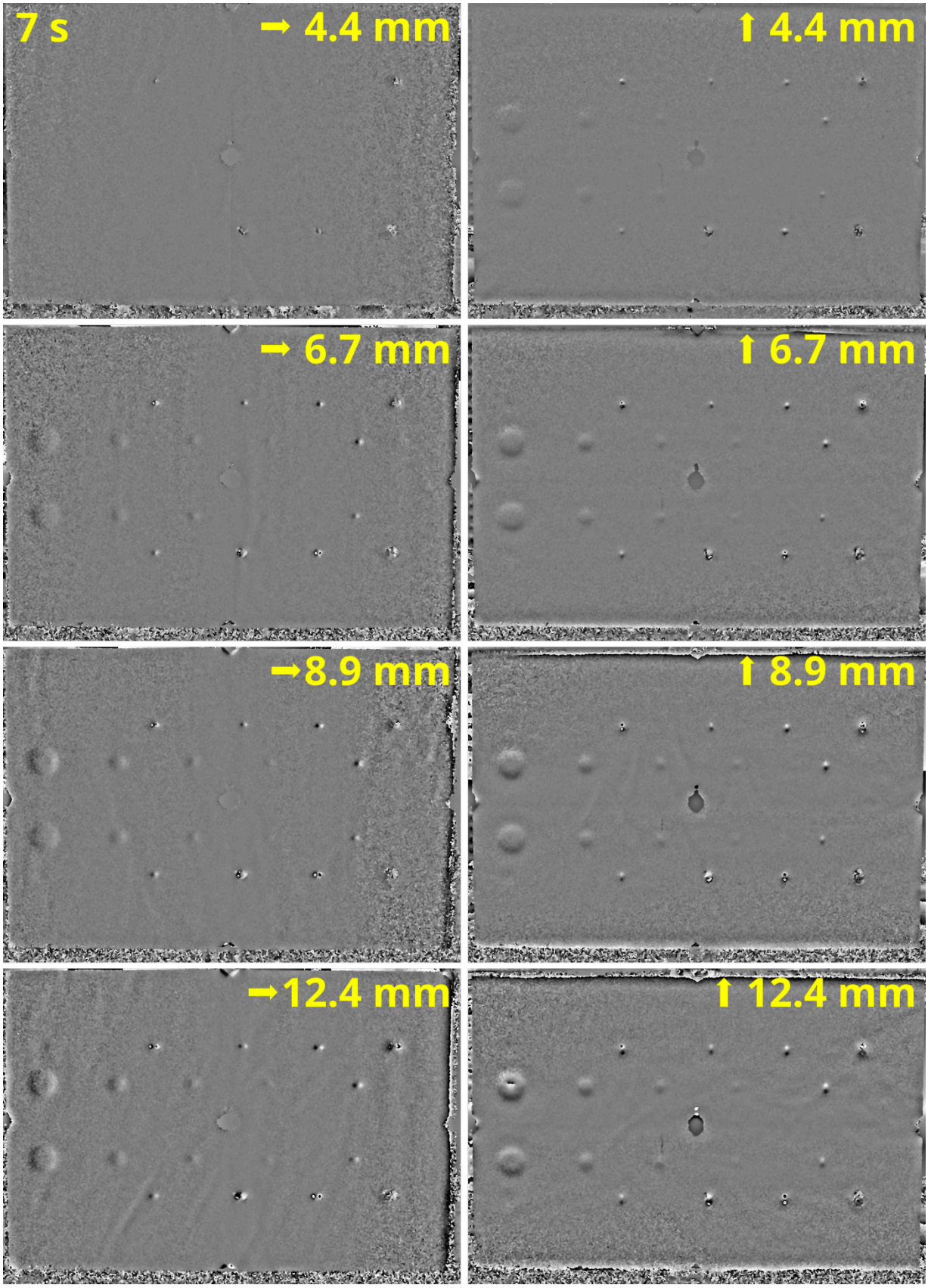

Figure 27: Wrapped shearogram of panel NLR-C. Shear direction is indicated by arrows (left pictures horizontal shear, right pictures vertical shear) and magnitude in mm is specified. For all pictures a pulse length of 15 seconds is used, except for the shearogram in the top left

The results on panel NLR-C are summarized in the Figure 28. All impact locations can be detected using shearography once the pulse length and the shear vector are set high enough. All skin-to-core disbonds (HD1-4) can be detected, but require a larger pulse length for detection. None of the Teflon inserts (Tx,x) can be detected using shearography. This is the same results as for panel NLR-A2. The inserts are adhered to the composite material and do not change the mechanical stiffness enough to be detected. All other items not marked were not present in the sample anymore. The water from the water ingress locations has already been diffused/evaporated. The upper half of the specimen is covered by a copper wire mesh which does not have an influence on the detectability of the defects.

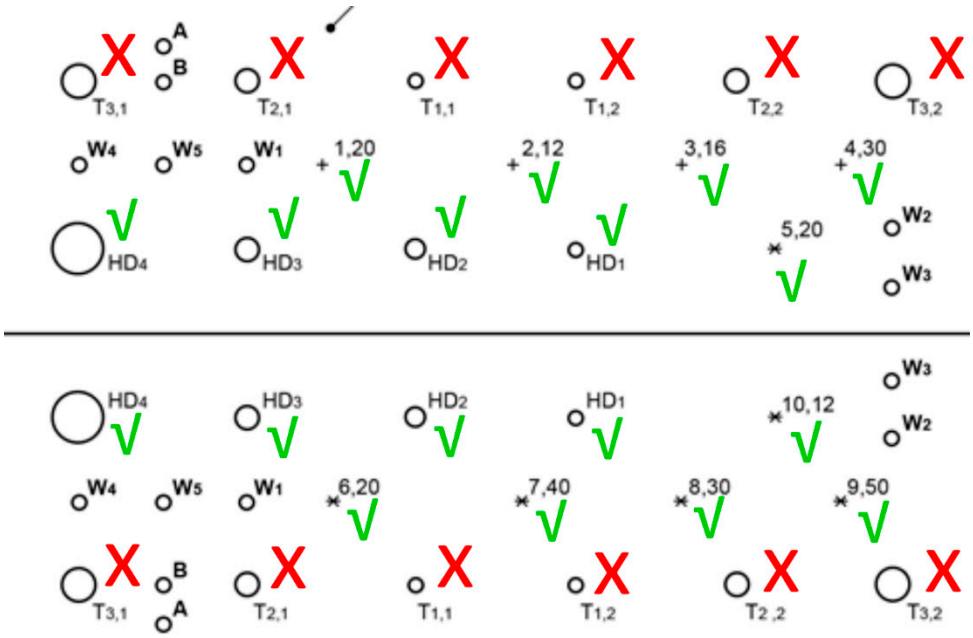

Figure 28: Results of panel NLR-C both for the vertical and horizontal shear. Artificial defects with a green check mark can be found using shearography. Artificial defects with a red cross cannot be found with shearography. Defects that contain not a check mark or a cross are not present on the sample anymore

8 Results from internship

The main goal of the initial research has been to create a clear baseline for future use of shearography as the complementary NDT technique. To achieve this goal, a literature review and practical tests have been executed. In order to formulate an answer to the main research question, this chapter will first treat the answers to the sub-questions stated in chapter 1:

What are the main theoretical benefits of shearography compared to other means of NDT currently used in aerospace?

To be able to assess the theoretical benefits of shearography, it is important to look at the downsides of the current means of NDT in aerospace. The disadvantages of the current methods of NDT resulting from a literature review are listed below (Table 3):

Table 3: Assessment on the benefits on shearography

	Shearography
High degree of operator skill required	-
Time-intensive	+
Requires contact with component	+
No analysis, just detection	+/-
Radiation hazard.	+
Sensitive to orientation of defect.	-
Only detects surface defects	+
Depth of inspection is limited.	-
Chemical disposal often required	+
Limited to certain materials	+
Not sufficient as a stand-alone method	+/-

+ Not applicable to shearography, +/- Semi-applicable (explanation below), - Applicable to shearography

The disadvantages are divided in two sections. The four main disadvantages listed on top in Table 3 are the factors that are the most valuable in the industry in terms of saving time and money. The semi-applicable disadvantages require a short explanation:

1. No analysis, just detection. While a shearogram won't give any information on the depth and the 3D geometry of a defect, it does give an idea on the 2D geometry as seen on the generic panel and its circular disbonds. So it is somewhat dependant on the type of defect.
2. Not sufficient as a stand-alone method. This depends on the type of defects that need to be found. For example shearography is ideally suited for sandwich structures since it can detect both impact damage, delaminations and skin-to-core disbonds. For monolithic composite material other NDI-techniques are needed to capture for example inserts.

Concluding, the following benefits are the theoretical result of using shearography; shorter inspection time, non-contact inspections, in-depth defect detection, no radiation or chemical hazards and no limitation in materials.

What are the requirements for shearography to be of sufficient added value?

The intended end goal is a multi-domain platform, incorporating multiple contactless NDT-methods. The following requirements are met using shearography as complementary NDT-method:

1. Non-contact measurements
2. Mobile setup
3. Field of view of around 1 m^2
4. Fast measurement time
5. Results that are distinctive from other methods incorporated in the multi-domain platform

What are the most suitable testing conditions for shearography, with the possible future user in mind?

As a result of the practical tests, some of the limitations of shearography have become apparent. A large factor that relates to the testing condition is the requirement for a relatively stable setup for the component. Although shearography was initially developed to reduce the effect of vibrations in comparison to ESPI, relative vibrational differences between the camera setup and the object under inspection still distort the shearogram and render the results unusable.

With the possible future user in mind, it is therefore essential to keep vibrations in mind in creating the most suitable testing conditions. The ideal situation would be to have the camera/laser setup and the setup meant to clamp the component under inspection on steady structures.

What are the practical capabilities of shearography when looking at various composite material properties and different types of defects?

The practical capabilities have become apparent after the analysis of the practical test results.

Although finding the optimal settings every time a new component is inspected consumes a lot of time, shearography is not limited by material properties. Also, dependent on those same material properties, the time required for a measurement is less than a minute, because a minimal local deflection in relation to the global deflection is needed for a result.

When increasing the FOV, the laser coverage becomes a critical factor in obtaining a usable end result. This increases the adjustment time considerably. However, after fine tuning, the minimal field of view of around 1 m2 as determined in the second sub-question can be achieved.

The setup used in this research, with the use of optical excitation, is able to show impact damage and disbonds. The water ingress and delamination in the generic panel are however not visible. This is as expected when considering the method of excitation.

Which of the theoretical benefits of shearography can be retraced from the practical research?

The answer to sub question 1 brings forth a list of theoretical benefits:

1. Shorter inspection times: yes, the inspection times relative to the current means of NDT in aerospace are indeed drastically lower.
2. Non-contact inspections: yes, shearography is indeed a contactless NDT-method.
3. The detection of sub-surface defects: yes, the results from the practical tests confirm that disbonds inside the component are clearly visible on the shearogram.
4. No radiation or chemical hazards: yes, the lasers in the setup are harmless and no chemical disposal is required during the tests.
5. No limitation of materials. No, this theoretical benefit is not confirmed by the practical research, due to the relatively small amount of different materials that were included in the test.

To what extent is the NDT-technique shearography suitable for future multi-domain aerospace maintenance on composite parts?

The answers to the sub-questions can now be used to answer the main research question. As an additional technique to the future multi-domain platform, it has the potential to be suitable dependent on application. It ticks all the boxes when looking at the requirements and in particular the superior ability to detect disbonds in honeycomb structures in a non-contact matter is a very valuable feature of the technique, since none of the other non-contact NDT methods in the multi-domain platform until now can do the same. The suitability for MRO applications in the end will highly depend on how stable (free of surrounding vibrations) the investigated objects can be investigated (minor vibrations lead to blurred or unusual images).

9 Conclusions

- Shearography is a fast and non-contact technique that is able to cover large surface areas.
- Settings for shearography are component dependant, and should be investigated for each different type of component.
- Generally speaking, longer pulse rates and higher shear vectors lead to better detectability of defects.
- Shearography is sensitive to vibrations, care should be taken to avoid excessive vibrations.
- All impact damage on both the solid laminate and honeycomb sample can be detected using shearography.
- There is no influence of the copper mesh on the detectability.
- All skin-to-core disbonds, through a 3 mm thick skin can be detected.
- None of the teflon inserts are detected using shearography. The teflon inserts are meant to simulate a delamination, but the inserts are still adhered to the laminate which does not results in a response for shearogaphy.
- The shearography method is an ideal partner in a multi-domain approach, e.g. in combination with thermography and 3D structural light scanning (not considered in this evaluation).

10 References

[1] J. Heida, “NLR memorandum AVGS-2018-004 "DCMC WP2 NDO methoden",” NLR, Amsterdam, 2018.

[2] E. Rademaker and D. H. J. Platenkamp, “NLR-CR-2019-100 Round Robin Test Results of Laser Ultrasonic System on Composite Panels,” NLR, Amsterdam, 2023.

[3] D. Platenkamp and H. Jansen, “NLR-CR-2018-365 Evaluation of in-service active thermography for composite structures,” NLR, Amsterdam, 2020.

[4] R. Lambrichs, “Investigation of Shearography as complementary NDT method,” Internship report InHolland, Amsterdam, 2020.

[5] J. Goodman, “Some fundamental properties of speckle,” *Journal of the Optical Society of America,* vol. 66, no. 11, pp. 1145-1150, 1967.

[6] Y.-K. Zhu, G.-Y. Tian, R.-S. Lu and H. Zhang, “A review of Optical NDT Technologies,” *Sensors,* vol. 11, no. 8, pp. 7773-7798, 2011.

[7] Y. Hung, “Shearography: A novel and practical approach for nondestructive inspection,” *Journal of Nondestructive evaluation,* vol. 8, pp. 55-67, 1989.

[8] D. Francis, R. Tatam and R. Groves, “Shearography technology and application: a review,” *Meas. Sci. Technol,* vol. 21, pp. 102001-102030, 2010.

[9] D. Francis, PhD thesis Surface strain measurement using pulsed laser shearography with fibre-optic bundles, Cranfield: Cranfield University, 2008.

[10] J. Gryzagoridis, “Vacuum excitation in shearographic NDT,” *Insight - Non-Destructive Testing and Condition Monitoring,* pp. 98-101, February 2007.

[11] Q. Kemao, S. Fangjun and W. Xiaoping, “Determination of the best phase step of the Carré algorithm in phase shifting interferometry,” *Meas. Sci. Technol,* vol. 11, no. 8, p. 2220, 2000.

[12] Edevis, “Shearography for non-destructive testing, measurement principle, excitation techniques, applications and how to,” Edevis, Stutgart, 2019.

Appendix A Specifications of Edevis shearography equipment

Camera

Camera:	Isi-Sys SE 2 with CCD sensor
Number of pixels	2452 x 2056 or 1226x1028 in binning mode
Frame rate	At 2452x2056 7Hz at 1226x1028 15 Hz
Resolution	12 bit
Interferometer	automatic calibration of beam splitter/mirrors (reference and shearing)

OTVIS excitation module

Name:	Edevis OTVIS 4000 Thermography system
Excitation source:	Halogen lamps 2 PCS 4kW
Filter :	Filter around 658 nm.

Lasers

Type	diode
Safety	Laser class 1 (no safety requirements)
Wave length	658 nm
Power	Using four arrays(5x100mW), total power 2W
Mode CW, Pulse	

Software

Software:	Edevis DisplayIMG 6.2.5.09 – Modul Shearovis

Dedicated to innovation in aerospace

Royal NLR - Netherlands Aerospace Centre

NLR operates as an objective and independent research centre, working with its partners towards a better world tomorrow. As part of that, NLR offers innovative solutions and technical expertise, creating a strong competitive position for the commercial sector.

NLR has been a centre of expertise for over a century now, with a deep-seated desire to keep innovating. It is an organisation that works to achieve sustainable, safe, efficient and effective aerospace operations.
The combination of in-depth insights into customers' needs, multidisciplinary expertise and state-of-the-art research facilities makes rapid innovation possible. Both domestically and abroad, NLR plays a pivotal role between science, the commercial sector and governmental authorities, bridging the gap between fundamental research and practical applications. Additionally, NLR is one of the large technological institutes (GTIs) that have been collaborating over a decade in the Netherlands on applied research united in the TO2 federation.

From its main offices in Amsterdam and Marknesse plus two satellite offices, NLR helps to create a safe and sustainable society. It works with partners on numerous programmes in both civil aviation and defence, including work on complex composite structures for commercial aircraft and on goal-oriented use of the F-35 fighter. Additionally, NLR helps to achieve both Dutch and European goals and climate objectives in line with the Luchtvaartnota (Aviation Policy Document), the European Green Deal and Flightpath 2050, and by participating in programs such as Clean Sky and SESAR.

For more information visit: **www.nlr.org**

Postal address
PO Box 90502
1006 BM Amsterdam, The Netherlands
e) info@nlr.nl **i)** www.nlr.org

Royal NLR
Anthony Fokkerweg 2
1059 CM Amsterdam, The Netherlands
p) +31 88 511 3113

Voorsterweg 31
8316 PR Marknesse, The Netherlands
p) +31 88 511 4444